Climate change impact on the hydrological cycle: instruments, uncertainty and applications
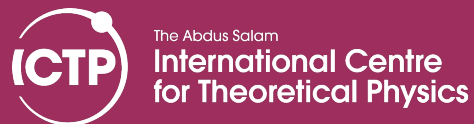
Erika Coppola & ICTP team

The Abdus Salam
**International Centre
for Theoretical Physics**

IAEA
International Atomic Energy Agency

unesco
United Nations
Educational, Scientific
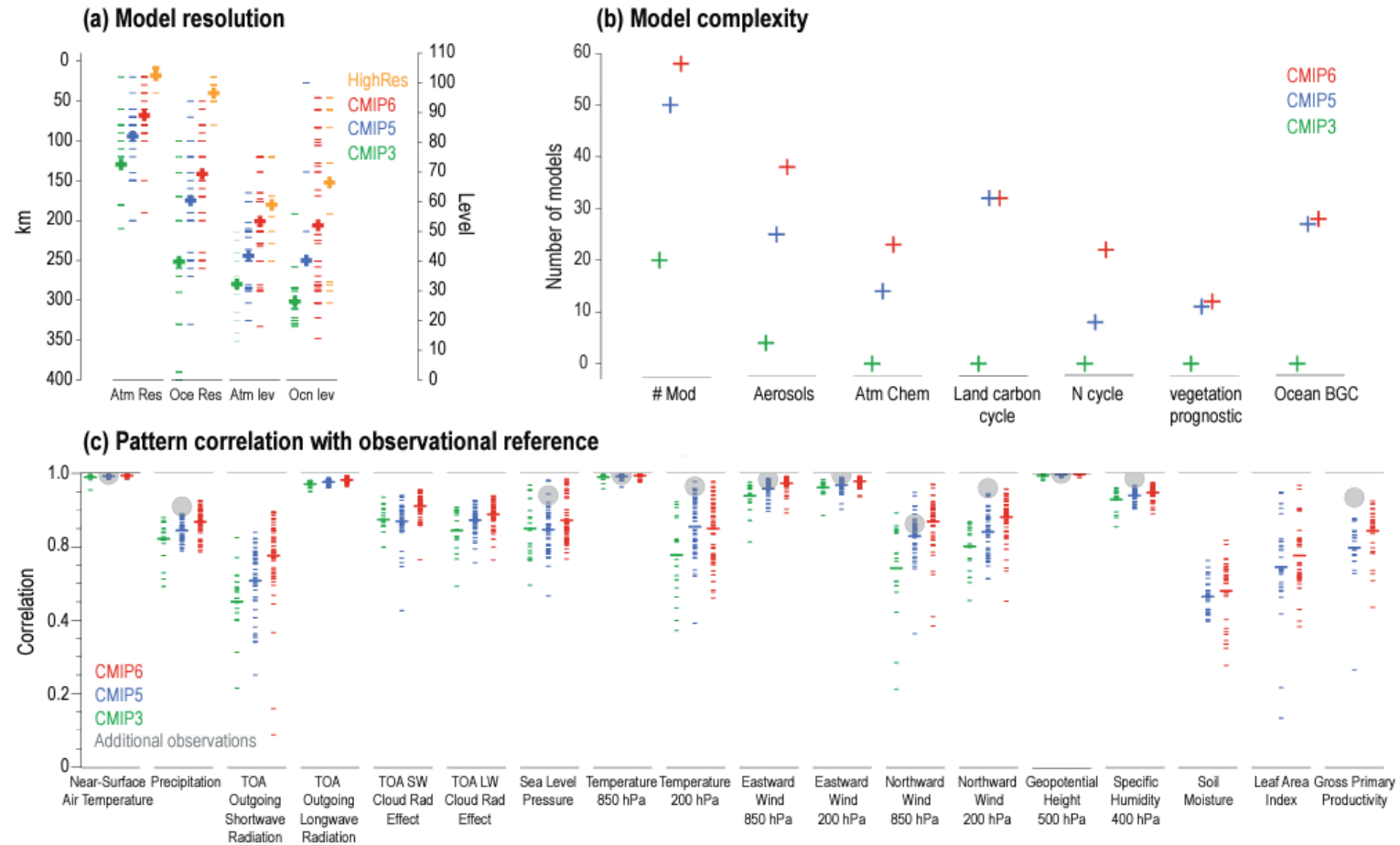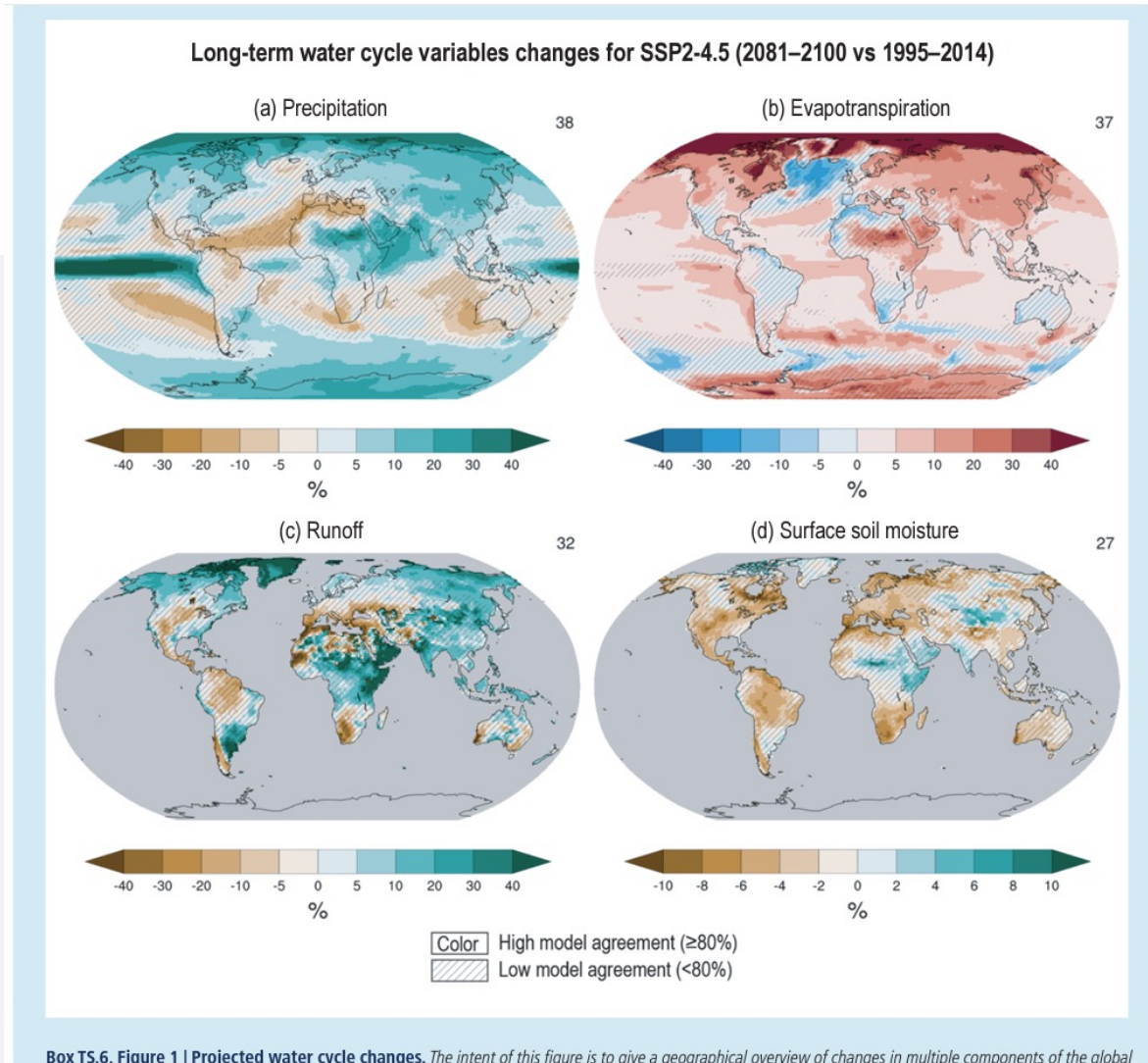and Cultural Organization

Global climate models

Figure TS.2 | Progress in climate models. *The intent of this figure is to show present improvements in climate models in resolution, complexity and representation of key*

Global climate models

Long-term water cycle variables changes for SSP2-4.5 (2081–2100 vs 1995–2014)

(a) Precipitation

(b) Evapotranspiration

(c) Runoff

(d) Surface soil moisture

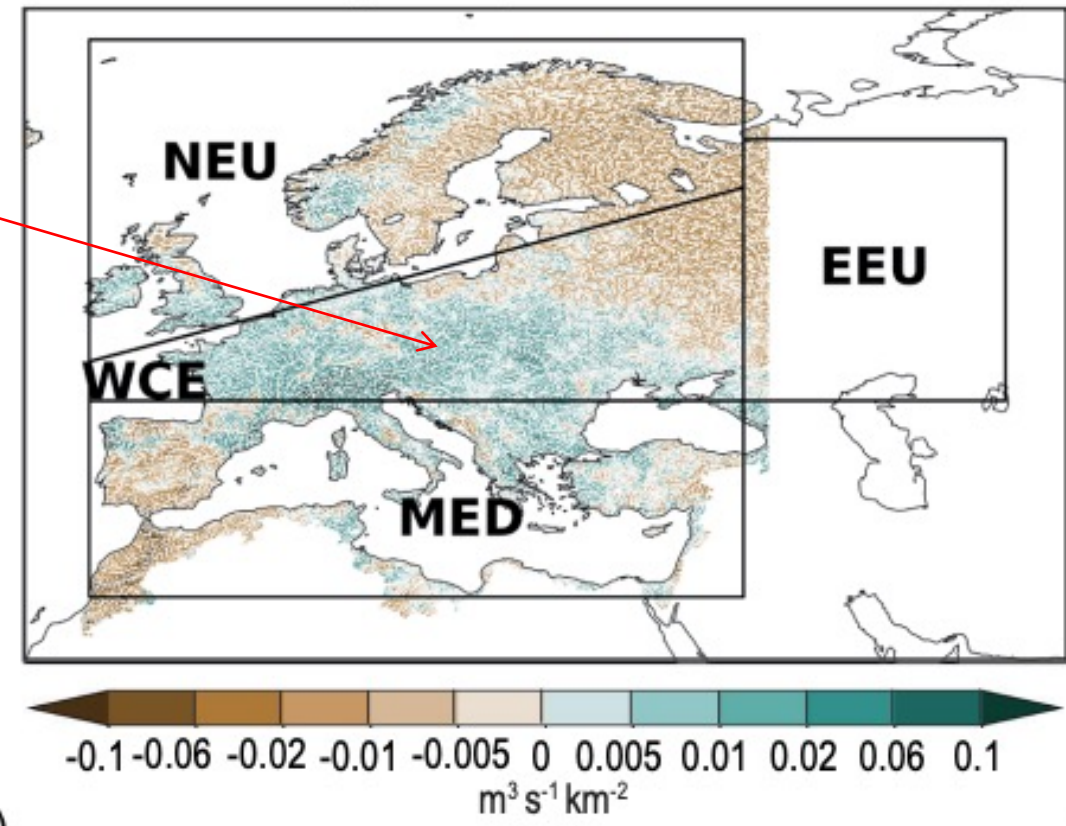Color — High model agreement (≥80%)
Low model agreement (<80%)

Box TS.6, Figure 1 | Projected water cycle changes. *The intent of this figure is to give a geographical overview of changes in multiple components of the global*
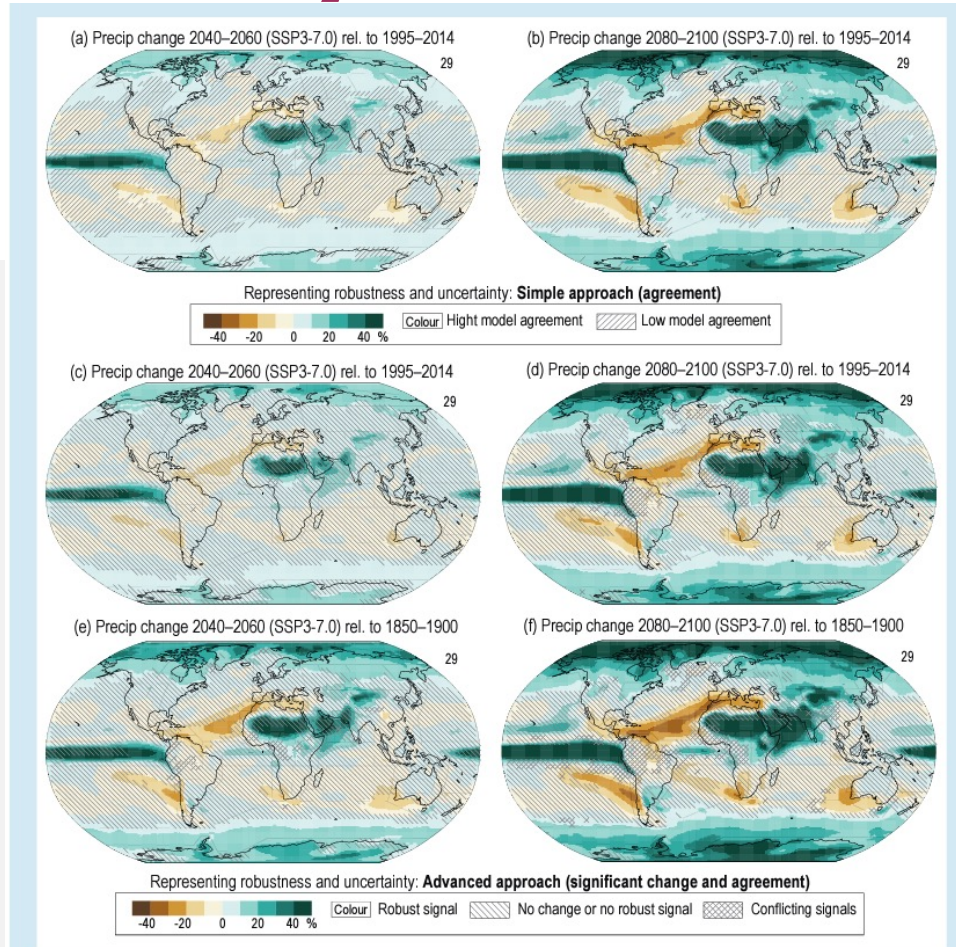
Global climate models

(c) Runoff
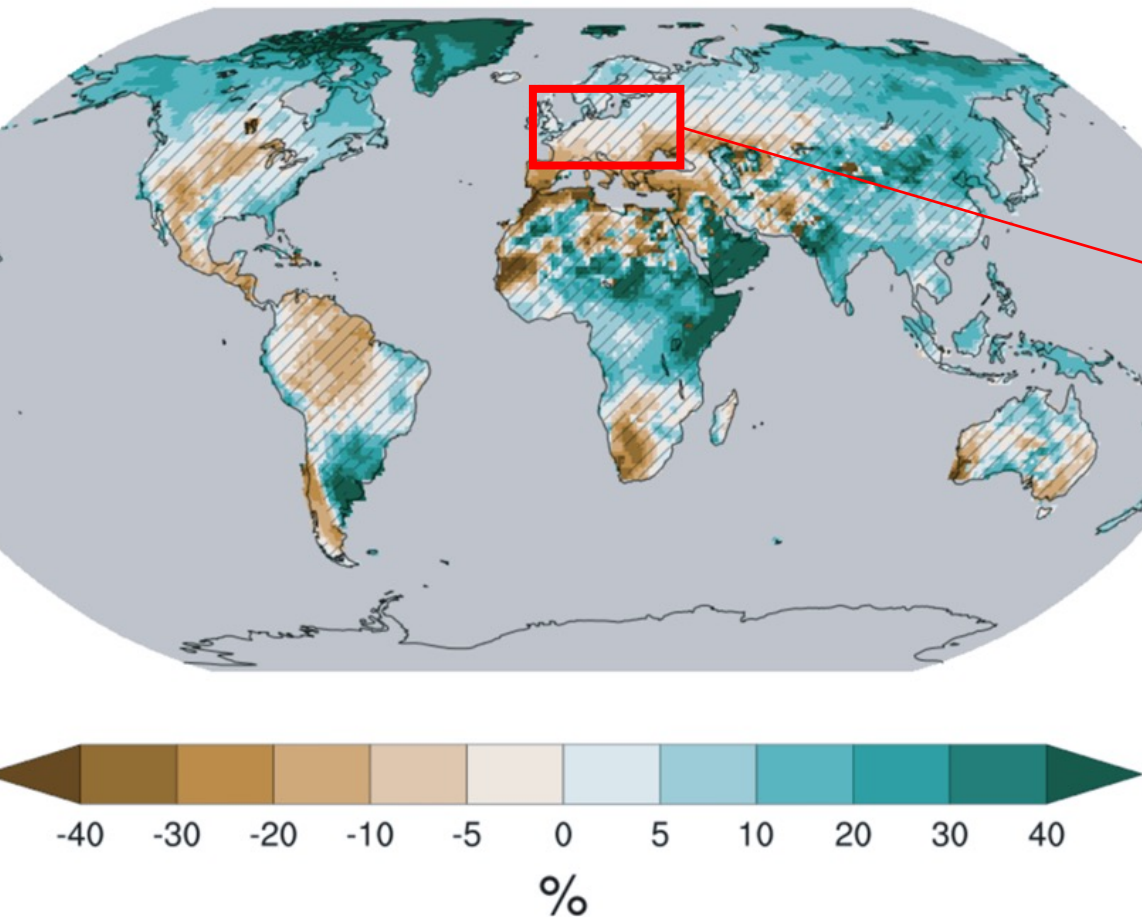
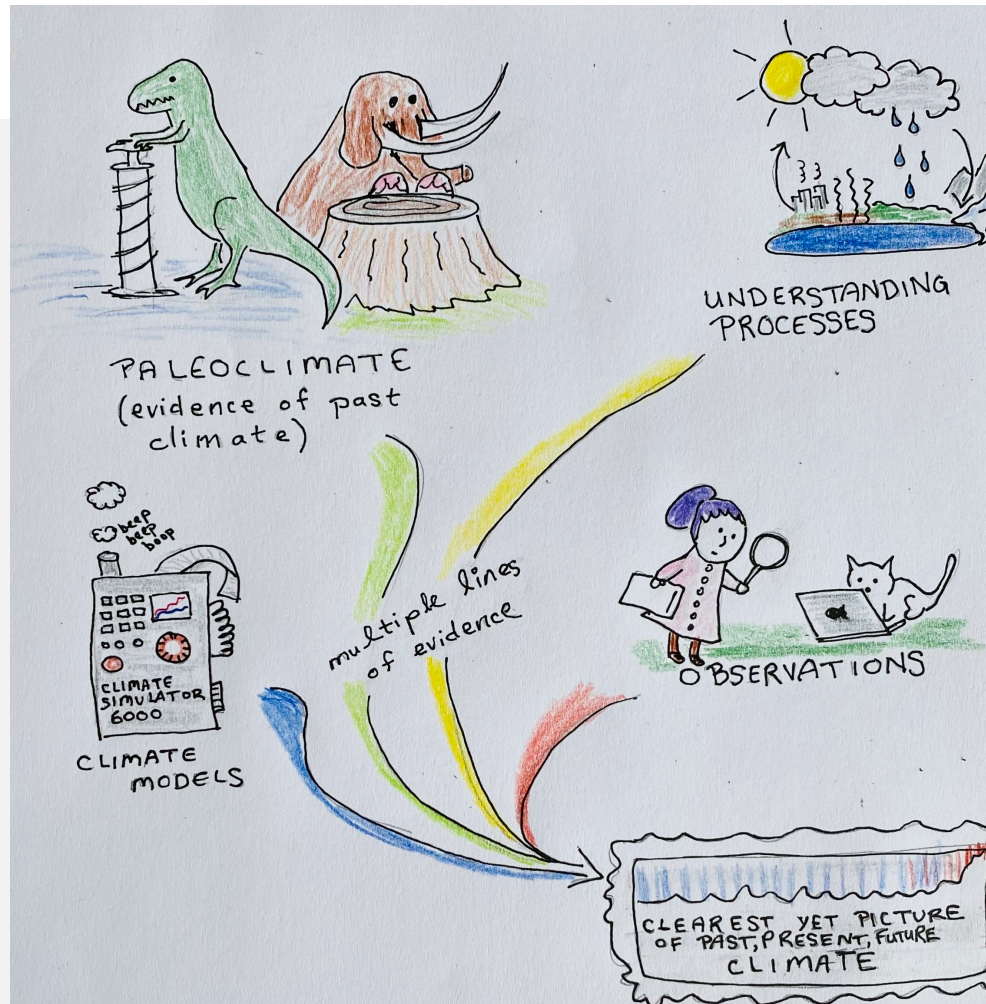(a) 1-in-100 year river discharge per unit catchment area by 2050, CORDEX RCP8.5
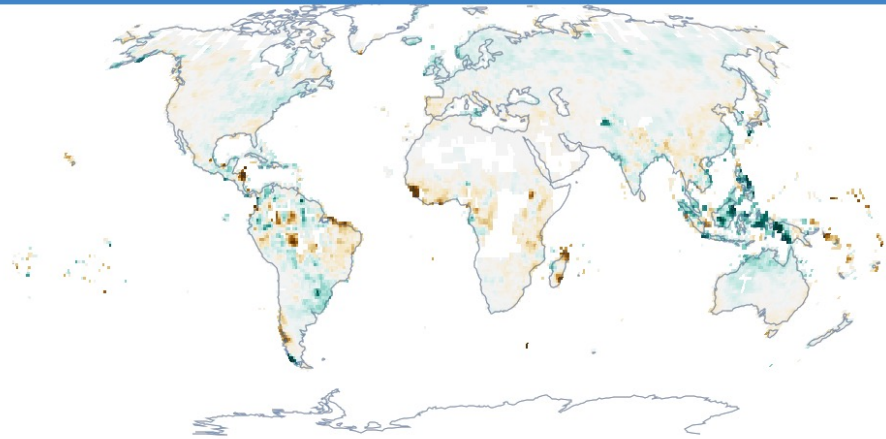
Model Uncertanty

Cross-Chapter Box Atlas.1, Figure 1 | Illustration of the simple, (a) and (b), and advanced, (c–f), approaches (B and C in Cross-Chapter Box Atlas.1, Table 1) for uncertainty representation in maps of future projections. Annual multi-model mean projected precipitation change (%) from CMIP6 for the period 2040–2060 (left) and 2080–2100 (right) relative to the baseline periods 1995–2014 (a–d) and 1850–1900 (e and f) under a high-emissions (SSP3-7.0) future. Diagonal and crossed lines follow the indications in Cross-Chapter Box Atlas.1, Table 1. Further details on data sources and processing are available in the chapter data table (Table Atlas.SM.15).

Gutiérrez, J.M., R.G. Jones, G.T. Narisma, L.M. Alves, M. Amjad, I.V. Gorodetskaya, M. Grose, N.A.B. Klutse, S. Krakovska, J. Li, D. Martínez-Castro, L.O. Mearns, S.H. Mernild, T. Ngo-Duc, B. van den Hurk, and J.-H. Yoon, 2021: Atlas. In Climate Change 2021: The Physical Science Basis. Contribution of Working Group I to the Sixth Assessment Report of the Intergovernmental Panel on Climate Change [Masson-Delmotte, V., P. Zhai, A. Pirani, S.L. Connors, C. Péan, S. Berger, N. Caud, Y. Chen, L. Goldfarb, M.I. Gomis, M. Huang, K. Leitzell, E. Lonnoy, J.B.R. Matthews, T.K. Maycock, T. Waterfield, O. Yelekçi, R. Yu, and B. Zhou (eds.)]. Cambridge University Press, Cambridge, United Kingdom and New York, NY, USA, pp. 1927–2058, doi:10.1017/9781009157896.021.
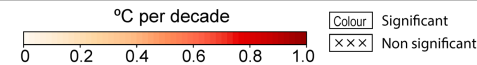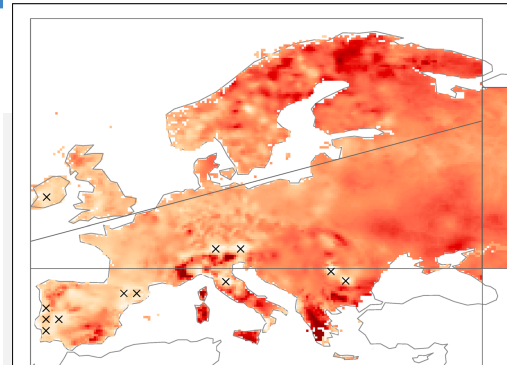
Climate Change robust assessment
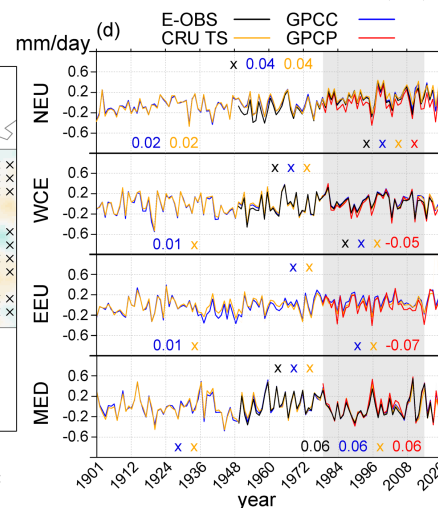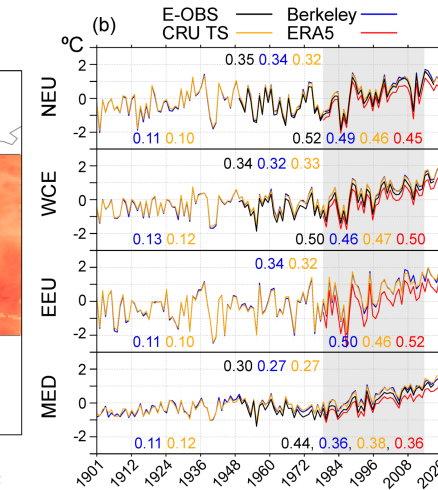## Multiple lines of eveidnece

Observed Trend global and regional
Uncertainty

(a) E-OBS annual Temperature (trends, 1980-2015)

°C per decade
0   0.2   0.4   0.6   0.8   1.0

Colour — Significant
××× — Non significant

(b) E-OBS, CRU TS, Berkeley, ERA5

(PR) – Trend (mm/day per decade)
ations)

Significant
Non significant

(c) E-OBS annual precipitation (trends, 1980-2015)

mm/day per decade
-0.4 -0.2   0   0.2   0.4

Colour — Significant
××× — Non significant

(d) E-OBS, CRU TS, GPCC, GPCP

Observed Trend ~~estimates and regional~~
Uncertainty

Process understanding and climate projections

Mediterranean summer warming
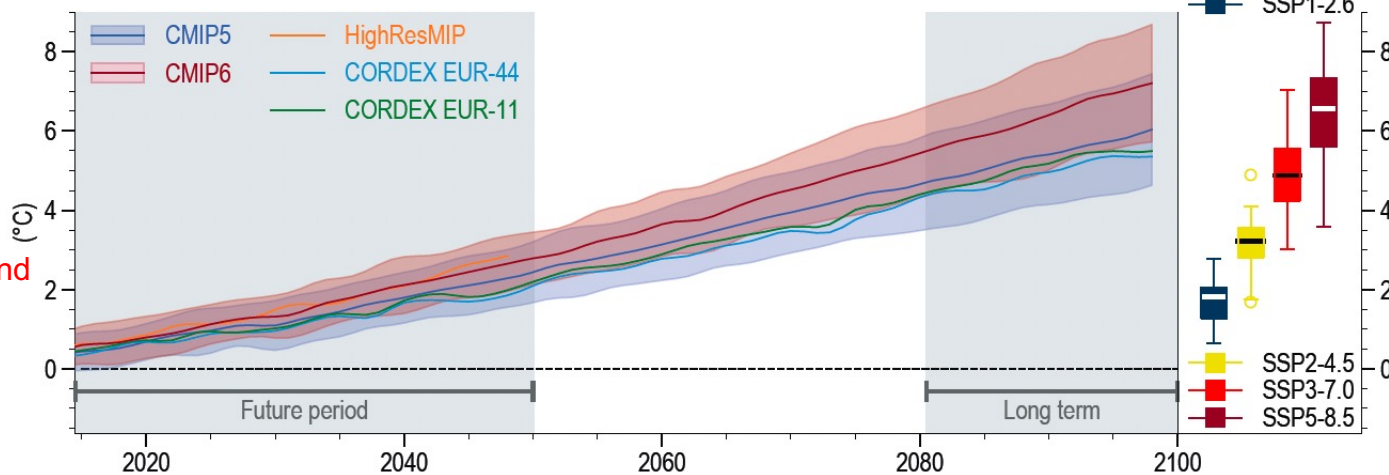
Observational evidence

Models can reproduce OBS

Process understanding

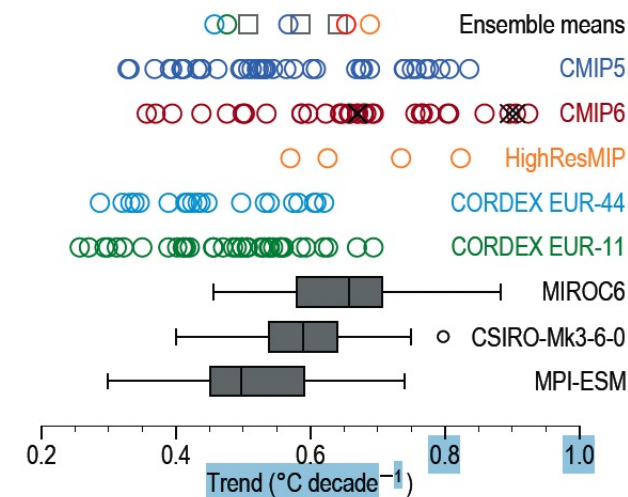Model projections agree and are consistend with OBS

(a) Projected Mediterranean temperature anomalies
Baseline period is 1995-2014

(b) Temperature trend distribution
Future period (2015-2050)

There is *very high confidence* (high agreement, robust evidence) that the **Mediterranean region has experienced a summer temperature increase in recent decades** that is faster than the increase for the Northern Hemisphere summer mean.

There is also *very high confidence* (high agreement, robust evidence) that the **projected Mediterranean summer temperature increase will be larger than the global warming level**, with an increase in the frequency and intensity of heatwaves.
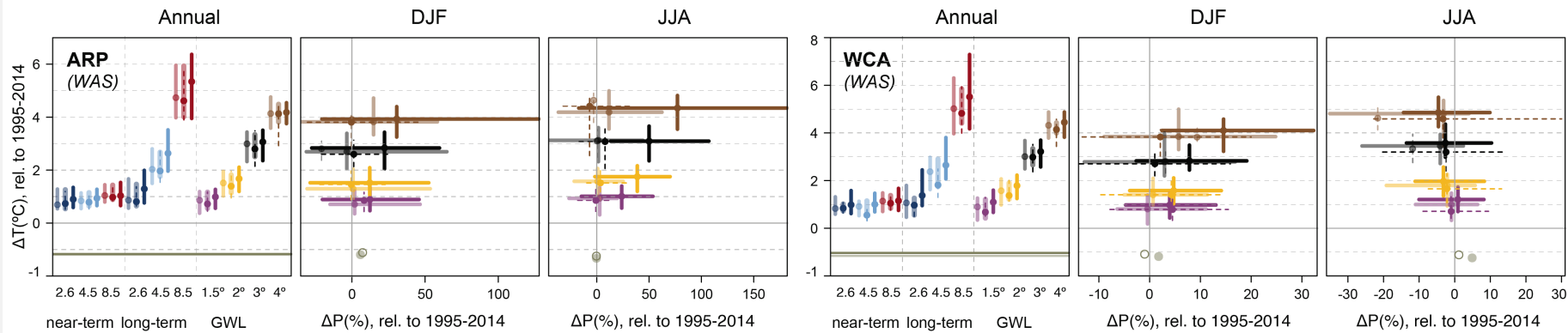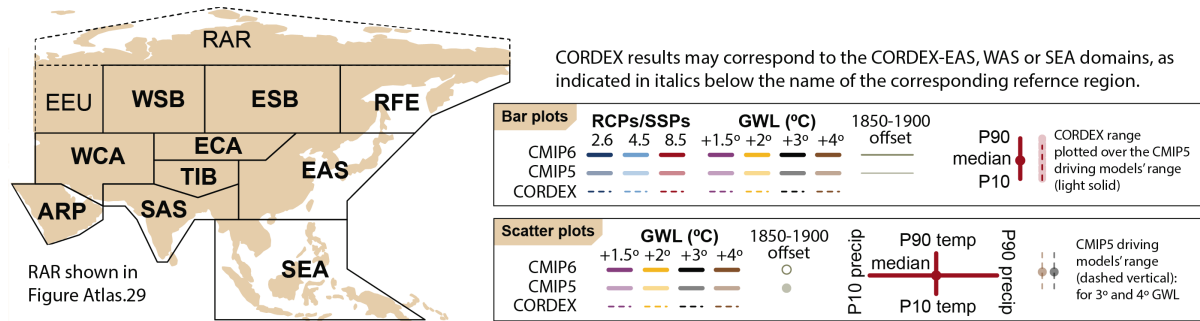
AR6 WGI-Chapter 10, **Figure 10.20-10.21**
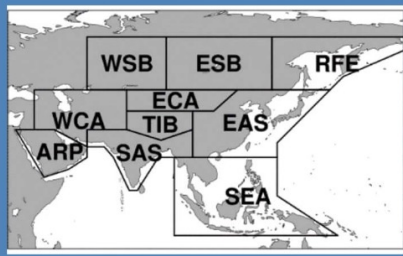
Robust climate change signal

Robust climate change signal

Region	Heat and Cold				Wet and Dry								Wind				Snow and Ice						Coastal and Oceanic				Other		
	Mean air temperature	Extreme heat	Cold spell	Frost	Mean precipitation	River flood	Heavy precipitation and pluvial flood	Landslide	Aridity	Hydrological drought	Agricultural and ecological drought	Fire weather	Mean wind speed	Severe wind storm	Tropical cyclone	Sand and dust storm	Snow, glacier and ice sheet	Permafrost	Lake, river and sea ice	Heavy snowfall and ice storm	Hail	Snow avalanche	Relative sea level	Coastal flood	Coastal erosion	Marine heatwave	Ocean acidity	Air pollution weather	Atmospheric CO_2 at surface	Radiation at surface
Arabian Peninsula (ARP)	●	●	●																				●		1	●			●	
West Central Asia (WCA)	●	●	●		5																		●		1,2	●			●	

5. Medium confidence of decreasing in summer and increasing in winter.

● Already emerged in the historical period (*medium* to *high confidence*)

● Emerging by 2050 at least in scenarios RCP8.5/SSP5-8.5 (*medium* to *high confidence*)

● Emerging after 2050 and by 2100 at least in scenarios RCP8.5/SSP5-8.5 (*medium* to *high confidence*)

High confidence of decrease	Medium confidence of decrease	Low confidence in direction of change	Medium confidence of increase	High confidence of increase	Not broadly relevant

Dynamical downscaling
Ensemble approach for uncertainty estimate

(a) Multi−model ensemble (MME)
One simulation of the time evolution of Q per model, with internal variabiliy

(b) Initial condition ensemble (ICE)
Multiple simulations of Q from one model, differing by initial conditions only

(c) Perturbed parameter ensemble (PPE)
Systematic perturbation of parameter(s) affecting Q, within one model

IPCC AR6 WGI Figure1.21 | Illustration of common types of model ensemble, simulating the time evolution of a quantity Q (such as global mean surface temperature)

Internal Variability
Scenario uncertainty
Model uncertainty

Decadal temperature - Global

Decadal temperature – UK
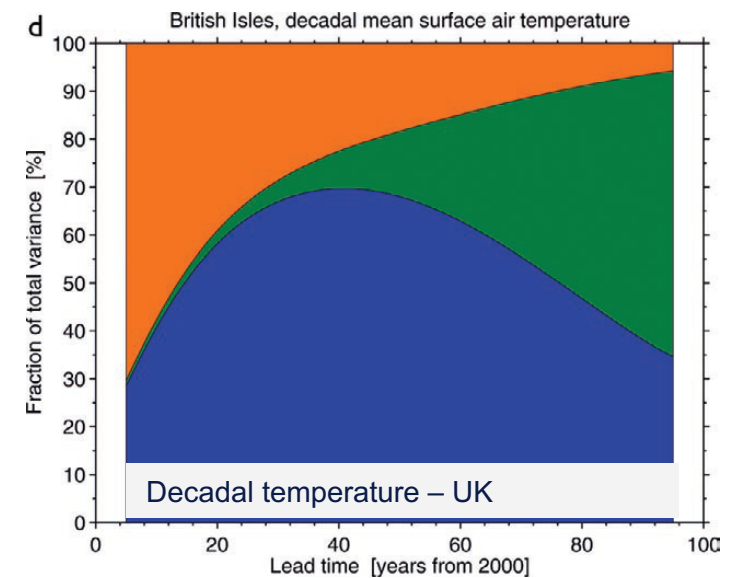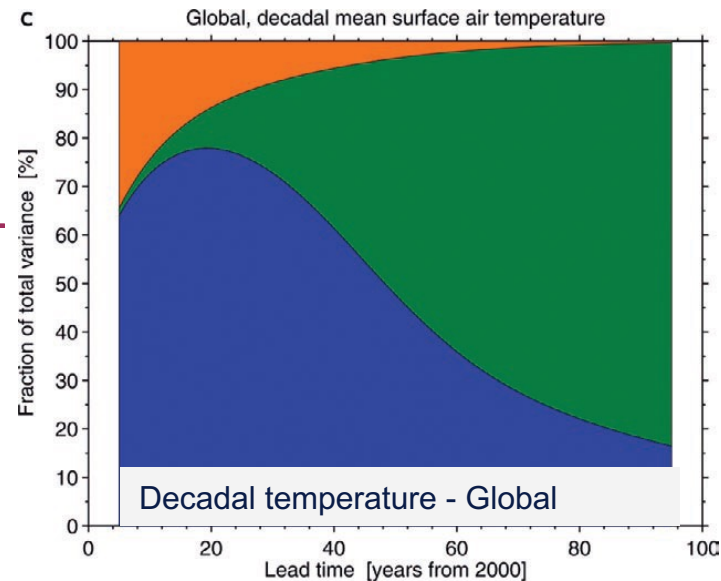
Hawkins and Sutton 2009

12

Methodology

To simulate the river discharge we made use of a river routing model derived from a distributed hydrological model (CHyM). The CHyM model has been already coupled (off-line and on-line) with an RCM to simulate the river discharge of the Italian Po river (Coppola et al. 2014) and that of the South Asia region (Di Sante et al. 2019).

Climate Model
(Calculates the total runoff for each land point)

Total runoff →

River Routing Model
(Calculates the river discharge for each river point of the hydrological model grid)

Yearly peak discharge →

GEV
(We fit the 100 year return period of a Gumbel distribution **Q100**)

0.11° (RCM)
0.25° - 1.5° (CMIP6)
0.5° - 2.5° (CMIP5)

Regridding to river grid →

0.06°
(CHyM)
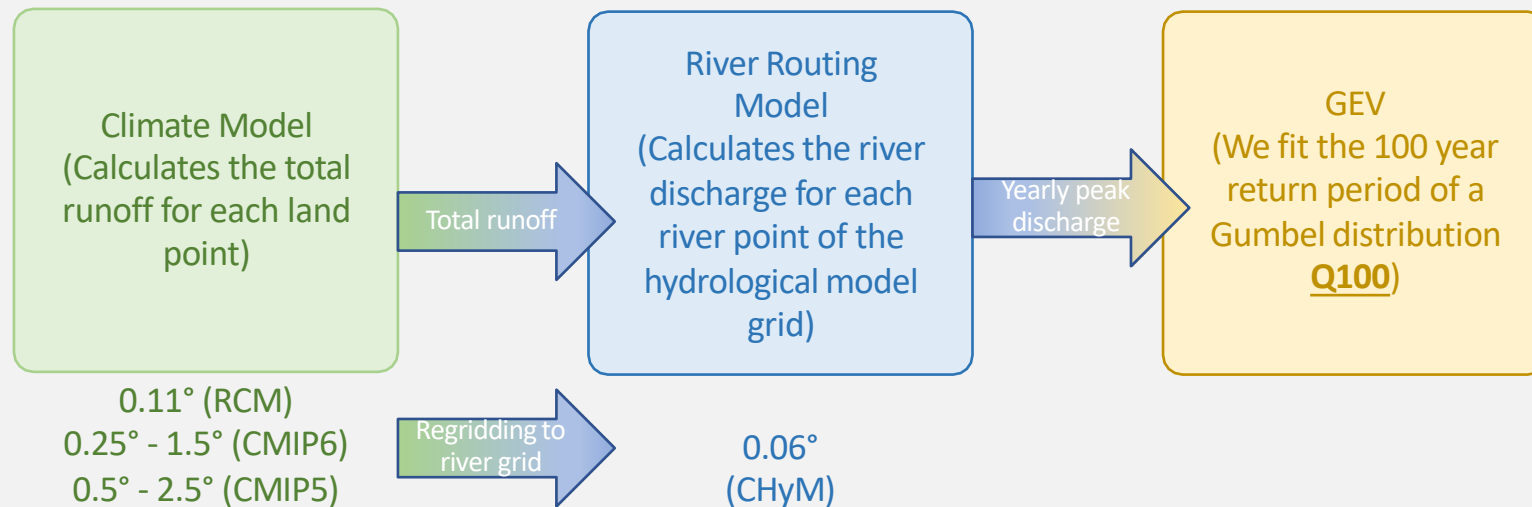
Methodology
Euro-CORDEX RCM

RCM	Driving Model	ens	Experiments
CLMcom-CCLM4-8-17	CCCma-CanESM2	r1	his, rcp85
CLMcom-CCLM4-8-17	CNRM-CERFACS-CNRM-CM5	r1	his, rcp85
CLMcom-CCLM4-8-17	ICHEC-EC-EARTH	r12	his, rcp85, rcp26
CLMcom-CCLM4-8-17	MIROC-MIROC5	r1	his, rcp85
CLMcom-CCLM4-8-17	MOHC-HadGEM2-ES	r1	his, rcp85
CLMcom-CCLM4-8-17	MPI-M-MPI-ESM-LR	r1	his, rcp85
CLMcom-ETH-COSMO-crCLIM-v1-1	MPI-M-MPI-ESM-LR	r1	his, rcp85
CNRM-ALADIN63	CNRM-CERFACS-CNRM-CM5	r1	his, rcp85, rcp26
CNRM-ALADIN63	MOHC-HadGEM2-ES	r1	his, rcp85
DMI-HIRHAM5	CNRM-CERFACS-CNRM-CM5	r1	his, rcp85
DMI-HIRHAM5	ICHEC-EC-EARTH	r12	his, rcp85
DMI-HIRHAM5	ICHEC-EC-EARTH	r1	his, rcp85
DMI-HIRHAM5	ICHEC-EC-EARTH	r3	his, rcp85, rcp26
DMI-HIRHAM5	MOHC-HadGEM2-ES	r1	his, rcp85
DMI-HIRHAM5	NCC-NorESM1-M	r1	his, rcp85
GERICS-REMO2015	CCCma-CanESM2	r1	his, rcp85
GERICS-REMO2015	CNRM-CERFACS-CNRM-CM5	r1	his, rcp85
GERICS-REMO2015	ICHEC-EC-EARTH	r12	his, rcp85, rcp26
GERICS-REMO2015	MIROC-MIROC5	r1	his, rcp85, rcp26
GERICS-REMO2015	MOHC-HadGEM2-ES	r1	his, rcp85, rcp26
GERICS-REMO2015	MPI-M-MPI-ESM-LR	r3	his, rcp85
GERICS-REMO2015	NCC-NorESM1-M	r1	his, rcp85, rcp26

RCM	Driving Model	ens	Experiments
ICTP-RegCM4-6	MOHC-HadGEM2-ES	r1	his, rcp85, rcp26
ICTP-RegCM4-6	MPI-M-MPI-ESM-LR	r1	his, rcp85
IPSL-WRF381P	CNRM-CERFACS-CNRM-CM5	r1	his, rcp85
IPSL-WRF381P	NCC-NorESM1-M	r1	his, rcp85
KNMI-RACMO22E	CNRM-CERFACS-CNRM-CM5	r1	his, rcp85, rcp26
KNMI-RACMO22E	ICHEC-EC-EARTH	r12	his, rcp85, rcp26
KNMI-RACMO22E	ICHEC-EC-EARTH	r1	his, rcp85
KNMI-RACMO22E	ICHEC-EC-EARTH	r3	his, rcp85
KNMI-RACMO22E	MOHC-HadGEM2-ES	r1	his, rcp85, rcp26
KNMI-RACMO22E	MPI-M-MPI-ESM-LR	r1	his, rcp85
KNMI-RACMO22E	NCC-NorESM1-M	r1	his, rcp85
MPI-CSC-REMO2009	MPI-M-MPI-ESM-LR	r1	his, rcp85
MPI-CSC-REMO2009	MPI-M-MPI-ESM-LR	r2	his, rcp85
SMHI-RCA4	CNRM-CERFACS-CNRM-CM5	r1	his, rcp85
SMHI-RCA4	ICHEC-EC-EARTH	r12	his, rcp85, rcp26
SMHI-RCA4	ICHEC-EC-EARTH	r1	his, rcp85
SMHI-RCA4	IPSL-IPSL-CM5A-MR	r1	his, rcp85
SMHI-RCA4	MOHC-HadGEM2-ES	r1	his, rcp85, rcp26
SMHI-RCA4	MPI-M-MPI-ESM-LR	r1	his, rcp85, rcp26
SMHI-RCA4	MPI-M-MPI-ESM-LR	r3	his, rcp85
SMHI-RCA4	NCC-NorESM1-M	r1	his, rcp85, rcp26
UHOH-WRF361H	ICHEC-EC-EARTH	r12	his, rcp85

Table s1. The 44 regional climate simulations, their driving GCMs, ensembles and experiments used to force the routing model in this study

12463 years simulated

Methodology
CMIP5-6 GCMs

CMIP5	Ensemble	Experiment
CNRM-CM5	r1	his, rcp85, rcp26
CanESM2	r1,r2,r3,r4,r5	his, rcp85, rcp26
MIROC-ESM	r1	his, rcp85, rcp26
MIROC5	r1	his, rcp85, rcp26
MPI-ESM-LR	r1,r2,r3	his, rcp85, rcp26
MPI-ESM-MR	r1	his, rcp85, rcp26
NorESM1-M	r1	his, rcp85, rcp26

Table s2. The 13 CMIP5 simulations ensembles and experiments

4719 years simulated

CMIP6	Ensemble	Experiment
CanESM5	r1	his, ssp585
EC-Earth3	r1	his, ssp585, ssp126
GFDL-CM4	r1	his, ssp585
IPSL-CM6A-LR	r1	his, ssp585, ssp126
MIROC6	r1	his, ssp585, ssp126
MPI-ESM1-2-HR	r1	his, ssp585, ssp126
UKESM1-0-LL	r1	his, ssp585, ssp126

Table s3. The 7 CMIP6 simulations ensembles and experiments

2299 years simulated

Completed using three queues on the Argo cluster hosted at ICTP.

HPC cluster "ARGO"

- Processors: 1910 cores – Intel based
- Theoretical calculation power: 25 teraFLOPS and 2 teraFLOPS via accelerators (GPUs)
- Storage: ~1,150TB raw (high speed and archive)

Methodology

The high resolution grid of the CHyM model allows to reproduce a fine drainage network with small rivers also represented. This allows in the analysis to take into account also flash floods happening in small river catchments.
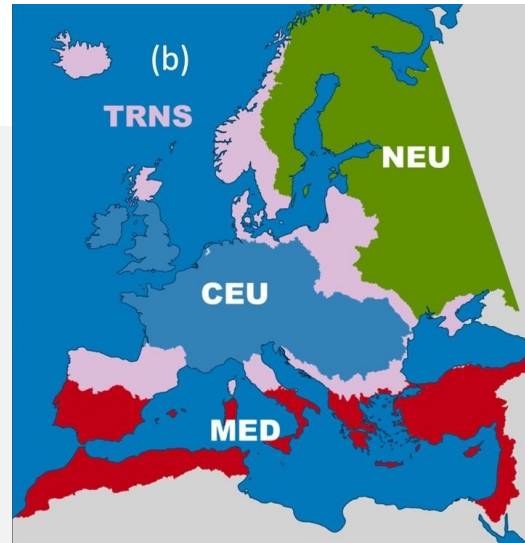
- **TRS: Transient**

- **NEU: North-East Europe CEU: Central Europe MED: Mediterranean**

Based on common characteristics and our results, we selected three main areas and a transient one as a buffer zone. In the analysis we tried to consider this three areas separately and compare the common characteristics and discuss the motivation of the observed and projected climatic signals.

- We considered three time periods and two different Representative Concentration Pathway (RCP; rcp2.6 and rcp8.5). The historic (**his**; 1985-2014), the mid future (**mid**; 2036-2065) and the far future periods (**far**; 2070-2099). The two RCP scenarios are selected based on their characteristics.
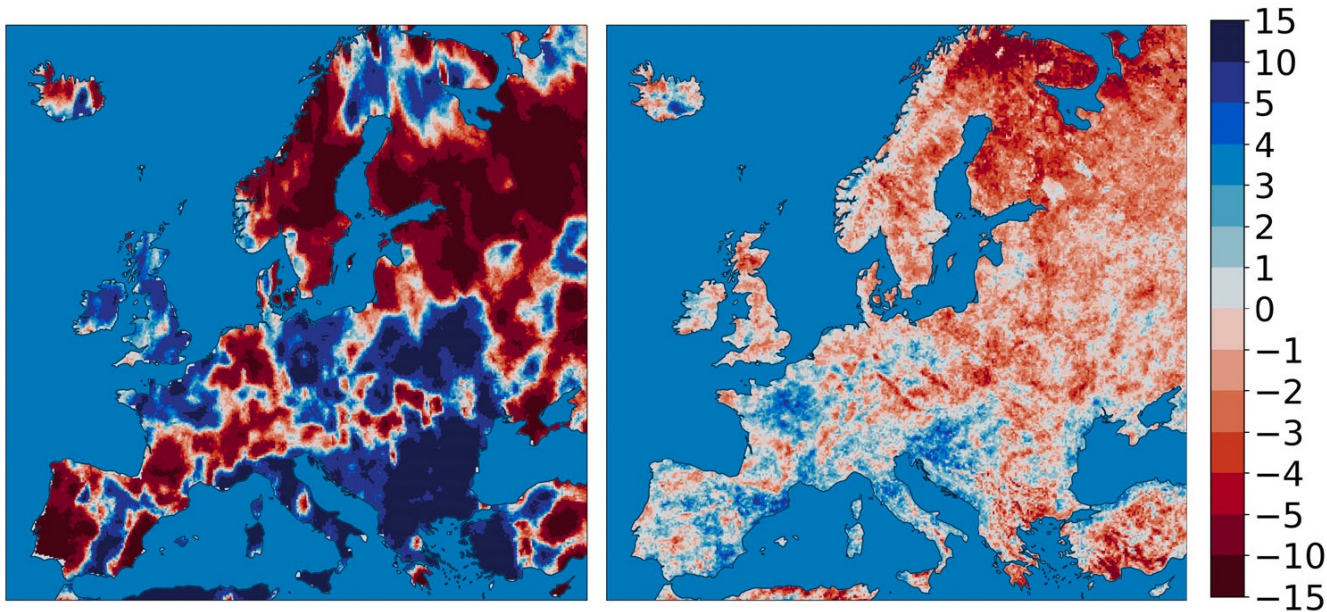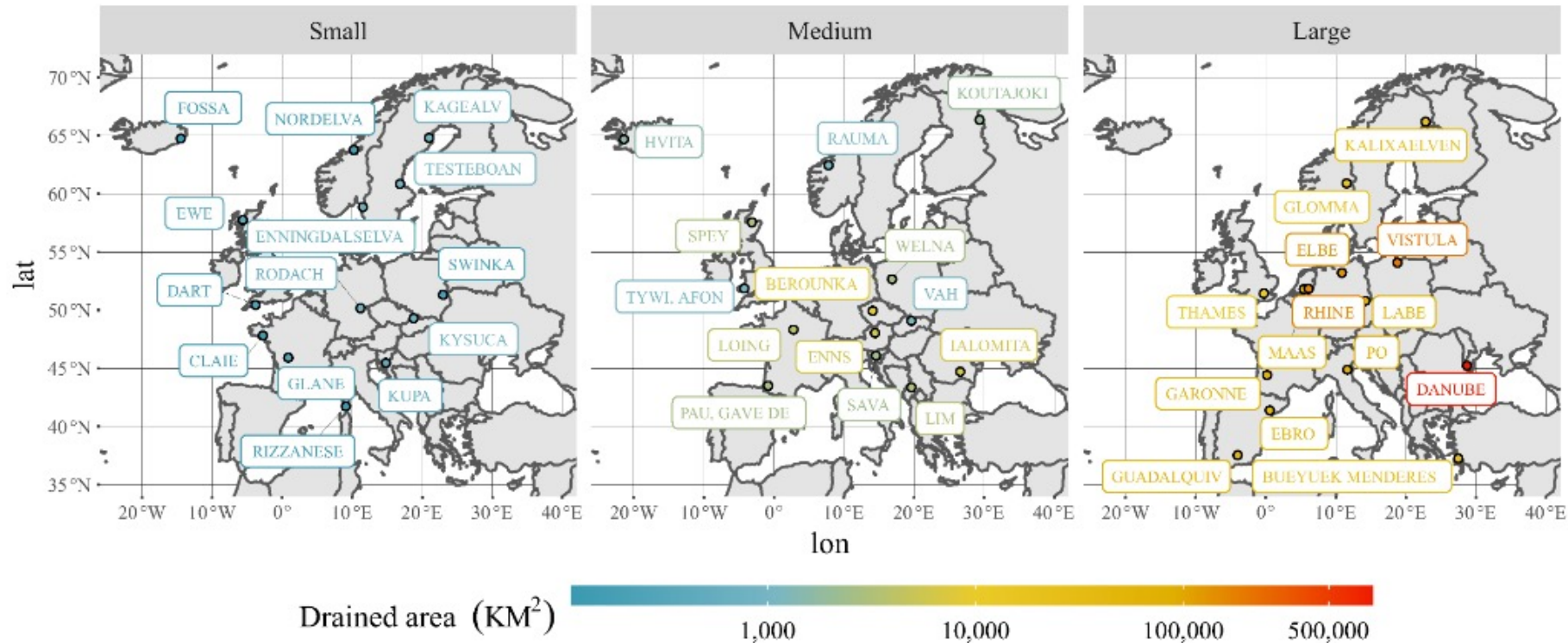
Methodology
Validation

FIGURE 6   Observed (left) and simulated (right) trend (% per decade) of annual maximum runoff for the 1985–2014 period

Di Sante, F., **Coppola**, E., & Giorgi, F. (2021). Projections of river floods in Europe using EURO-CORDEX, CMIP5 and CMIP6 simulations. *International Journal of Climatology*, *41*(5), https://doi.org/10.1002/joc.7014, 3203-3221.

Methodology
Validation

Methodology
Validation: mean bias

Validation : Mean runoff bias (%) for all the members of the EURO-CORDEX against the GRUN observation-based dataset for the 1985-2014 period
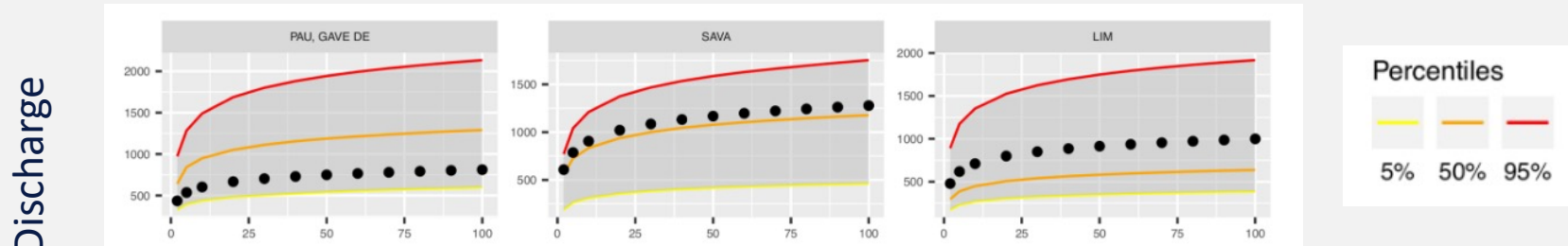
Methodology
Validation: flood-recurrence curves

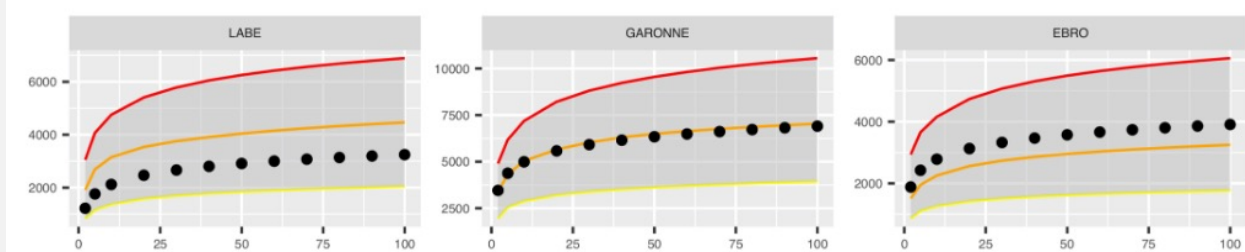European small (drained areas between 100 and 1,000 km2) river stations
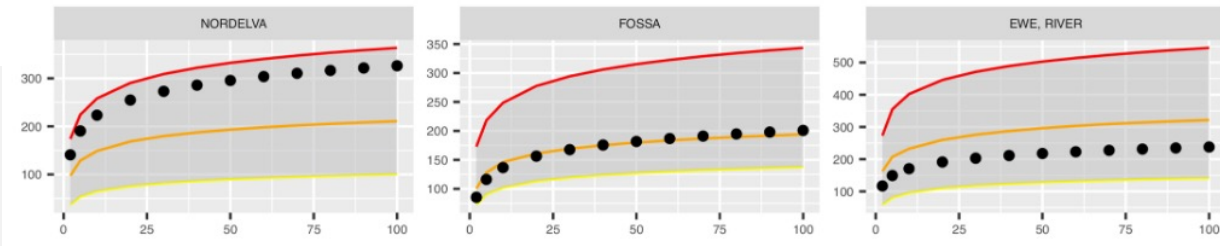
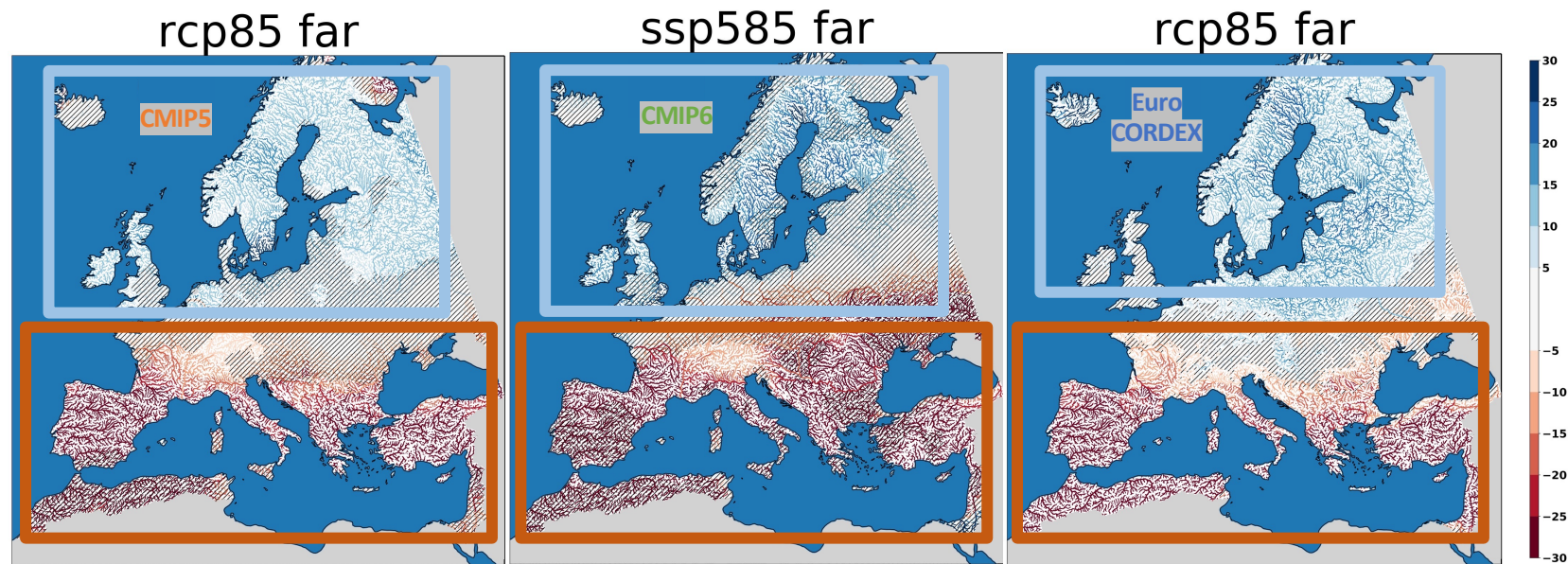European medium (drained areas between1,000 and 10,000 km2) river stations

European large (drained areas larger than10,000 km2) river stations

Discharge

Return Period (years)

# **Results**
Mean flow changes Far-His(%)

The three different simulation ensembles are in good agreement with each other. It can be observed a gradient from south to north. A strong decrease up to 30% on the 30 years mean can be observed on the MED region by the end of the century. A less marked increase (around 10-20%) can be instead observed over the high latitude region, in particular over the north-east.

The hatching represents areas where the change is not statistical significant at 0.05 level.

21

Results
Q100 changes for rcp85 (ssp585 CMIP5) - far
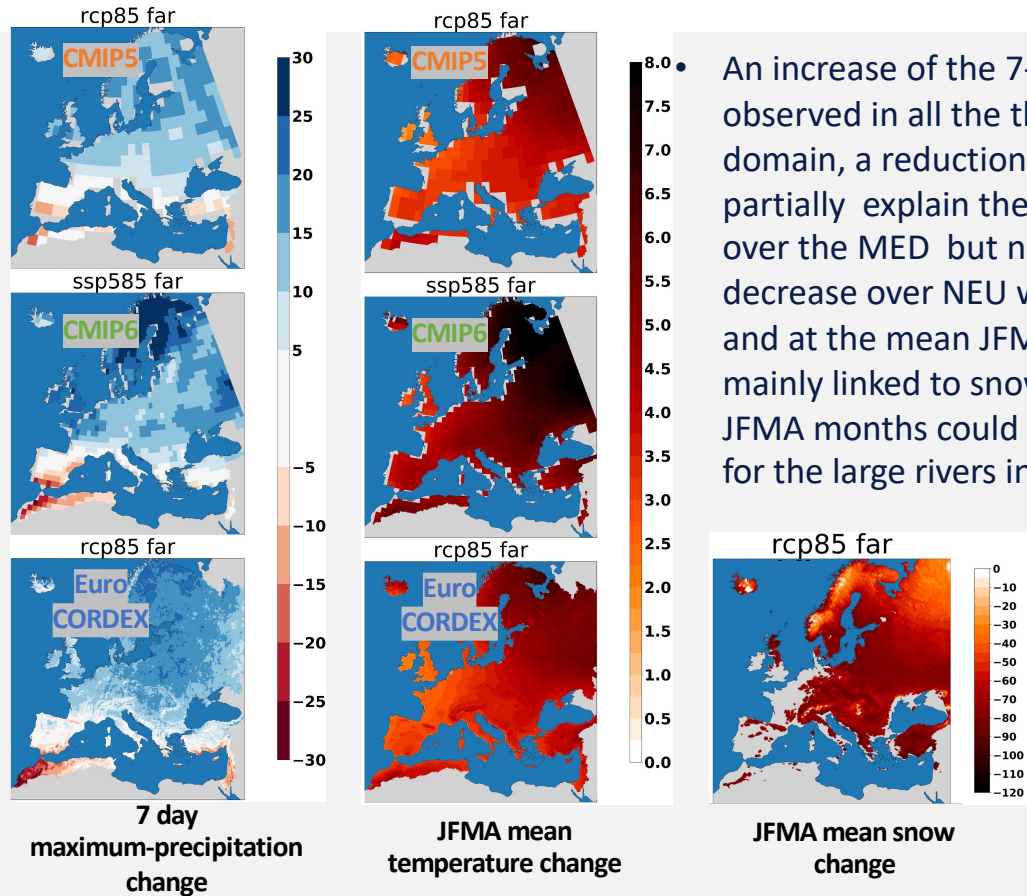

rcp85 far   ssp585 far   rcp85 far
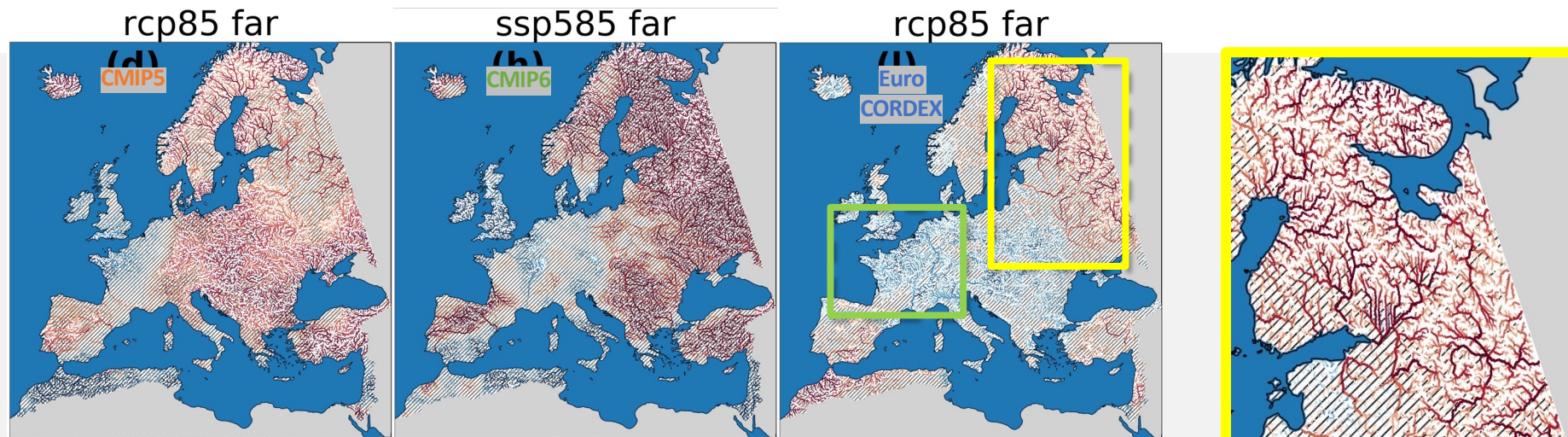
Over the NEU, a general decrease can be observed by the three ensembles. From the two zoomed boxes can be clearly seen as the strongest changes are related to the large rivers (median change of -19% against -4% for small rivers). On the other hand, if we focus on the CEU region, we can see as the greatest positive changes are related to middle and small rivers (median change of 19% against 11% for large rivers).

The hatching represents areas where the change is not statistical significant at 0.05 level

22

Results
Physical understanding

7 day maximum-precipitation change

**JFMA mean temperature change**

JFMA mean snow change

- An increase of the 7-day maximum precipitation change can be clearly observed in all the three ensemble in the central and north part of the domain, a reduction is instead observed on the south. This could partially explain the increase of flood risk over the CEU, the decrease over the MED but not the decrease over the NEU. To explain the decrease over NEU we need to look at the mean JFMA temperatures and at the mean JFMA snow changes. The floods in the NEU region are mainly linked to snow melt. A reduction of snow cover and thickness on JFMA months could be the reason of the robust decrease on floods risk for the large rivers in all the three ensembles.

23

Results
Physical understanding

The first think to notice is a larger uncertainties of CMIPs simulations compared to CORDEX, especially over the MED and NEU regions. The larger increases, as shown also in the spatial plots, are confirmed in this whisker's plots over the CEU region for CORDEX and small basins.

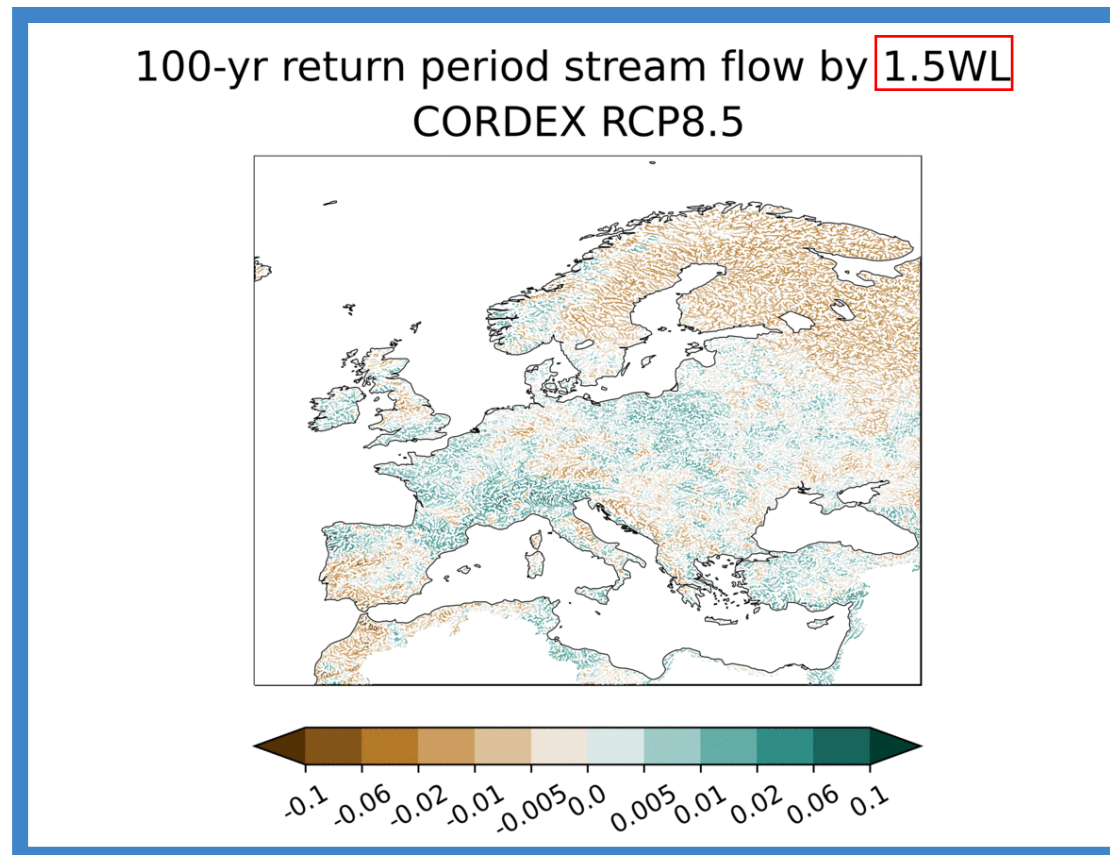The larger decreases are instead projected for NEU and MED for the large basins

24
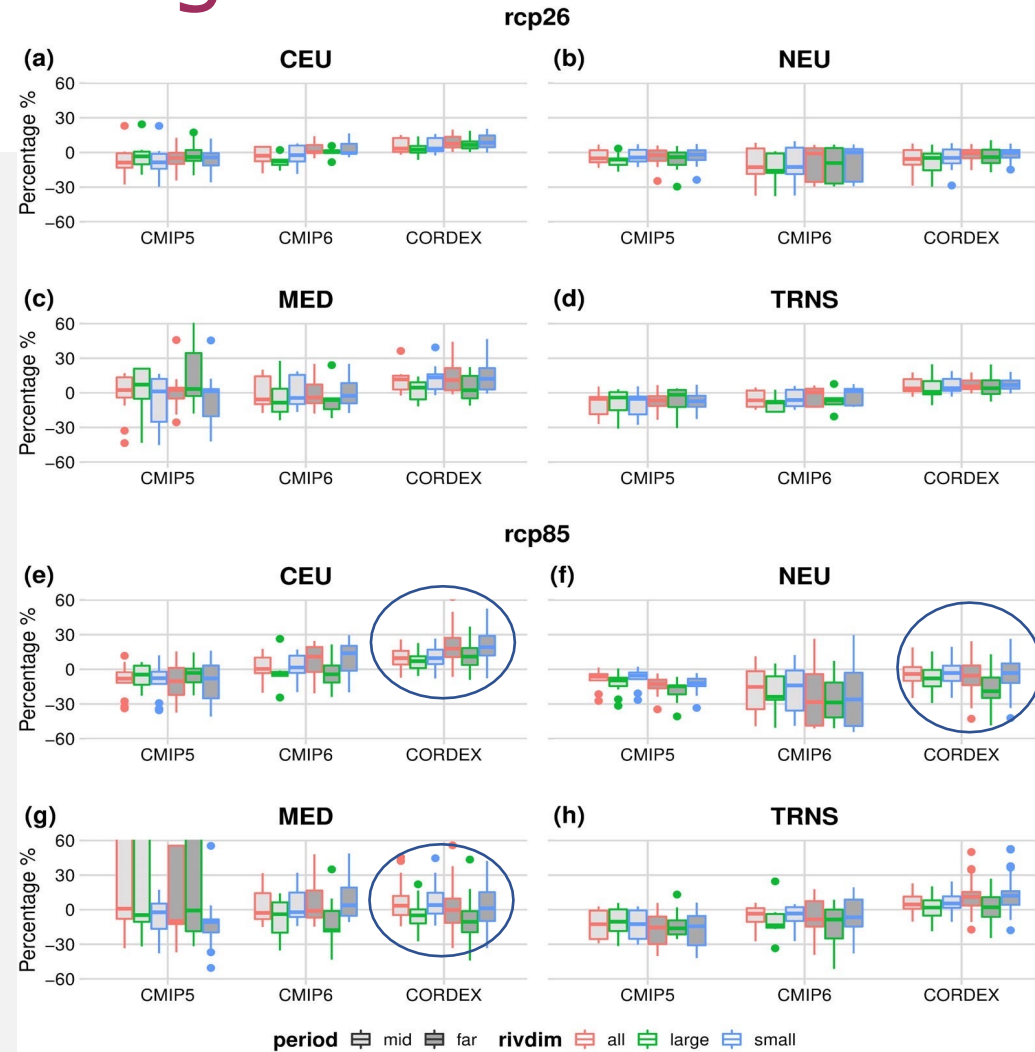
Results
What have we learned

- Results are in good agreement with the previous studies. Three main areas are highlighted. The MED where a decrease of flood risk is simulated by the end of the century. The CEU region where an increase of floods risk, probably linked to increase of extreme precipitation events. The NEU where the increase of temperature linked to global warming and the related less amount of snow accumulated during winter can lead to a decrease of the floods.

- The different underlying nature of the floods over the CEU and NEU regions could be the reason of the correlation between the intensity of the flood signal with the dimension of the river catchments. CEU much prone to flash floods and NEU much more sensitive to snow melt.

- This study is one of the largest hydroclimatic study ever with more than 160 hydroclimatic simulation completed. This gives the possibility to estimate the robustness of the climate change signal on floods hazard in Europe.

- The ever-increasing resolution and complexity of the RCMs allows the use of a simple and fast approach, without the needs of any bias correction to evaluate the flood risk signal linked to climate change.

- This allows to easily apply this approach to an even larger ensemble and to different domains (like the others CORDEX domains) without much computational expenses. (Di Sante et al. in preparation)

25

Results
Flood hazad as a function of the GWLs

100-yr return period stream flow by 1.5WL
CORDEX RCP8.5

-0.1 -0.06 -0.02 -0.01 -0.005 0.0 0.005 0.01 0.02 0.06 0.1

Changes in flood hazards would be more widespread at 2°C compared to 1.5°C global warming and even more widespread and/or pronounced for higher warming levels

Results

Future projections of river floods hazard over the multiple CORDEX-CORE domains

8 domains x 6 CORDEX x 2 projections = 96 simulations
from 1979 to 2100 (11616 simulated years)

CMIP5 rcp85	CMIP5 rcp26	CMIP6 ssp858	CMIP6 ssp126
BCC-CSM1.1	BCC-CSM1.1	ACCESS-CM2	ACCESS-CM2
CanESM2	CanESM2	BCC-CSM2-MR	BCC-CSM2-MR
CMCC-CM	CNRM-CM5	CanESM5	CESM2
CMCC-CMS	CSIRO-Mk3.6	CESM2	EC-Earth3
CNRM-CM5	FGOALS-G2.0	EC-Earth3	HadGEM3-GC31-LL
CSIRO-Mk3.6	GFDL-ESM2G	GFDL-CM4	HadGEM3-GC31-MM
FGOALS-G2.0	GFDL-ESM2M	HadGEM3-GC31-LL	INM-CM4-8
GFDL-ESM2G	MIROC-ESM	HadGEM3-GC31-MM	INM.INM-CM5-0
GFDL-ESM2M	MIROC5	INM-CM4-8	IPSL-CM6A-LR
INM-CM4	MPI-ESM-MR	INM.INM-CM5-0	KACE-1-0-G
MIROC-ESM	MPI-ESM-LR	IPSL-CM6A-LR	MIROC6
MIROC5	MRI-CGCM3	KACE-1-0-G	MIROC-ES2L
MPI-ESM-MR	NorESM1-M	MIROC6	MPI-ESM1-2-HR
MPI-ESM-LR		MIROC-ES2L	MPI-ESM1-2-LR
MRI-CGCM3		MPI-ESM1-2-HR	MRI-ESM2-0
MRI-ESM1		MPI-ESM1-2-LR	NorESM2-LM
NorESM1-M		MRI-ESM2-0	NorESM2-MM
		NorESM2-LM	UKESM1-0-LL
		NorESM2-MM	
		UKESM1-0-LL	

CORDEX-CORE	Driving GCM	Projection
GERICS-REMO2015	MOCH-HadGEM2-ES MPI-M-MPI-ESM-LR NCC-NorESM1-M	rcp26 rcp85
ICTP-RegCM4	MOCH-HadGEM2-ES MPI-M-MPI-ESM-MR NOAA-GFDL-GFDL-ESM2M	rcp26 rcp85

8 domains x 68 CMIPs = 544 simulations from 1979 to 2100
(65824 simulated years)

Results

Future projections of river floods hazard over the multiple CORDEX-CORE domains
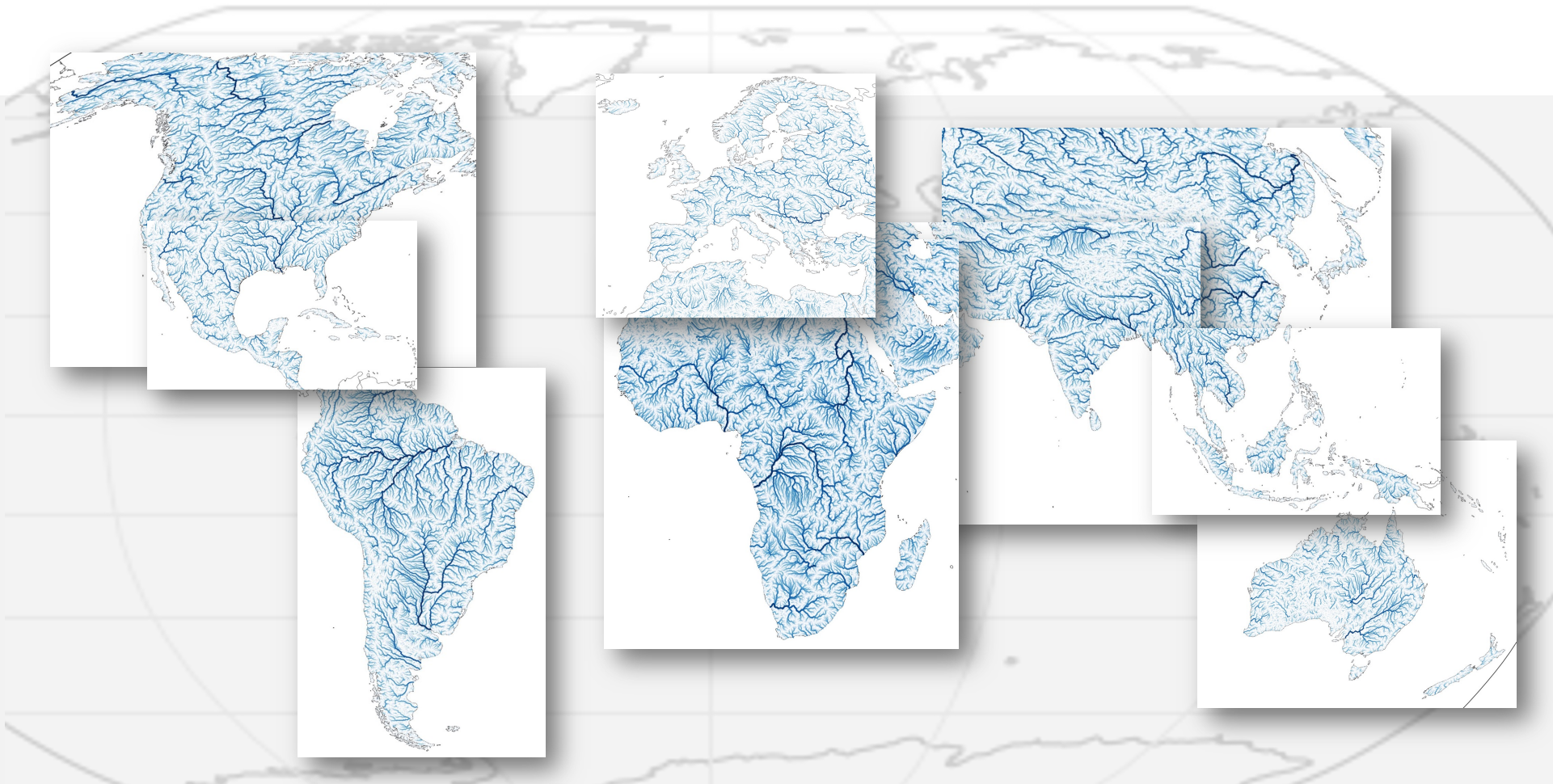
Results

Future projections of river floods hazard over the multiple CORDEX-CORE domains
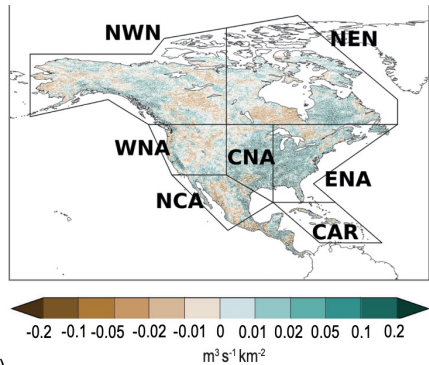
IPCC WGI AR6 CH12

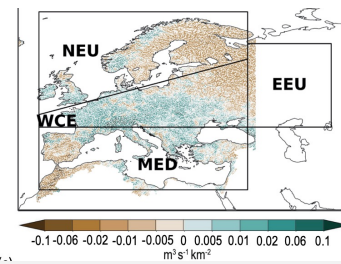Figure 12.10 | Projected changes in selected climatic impact-driver indices North America.

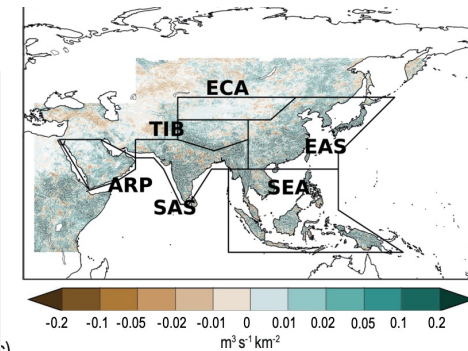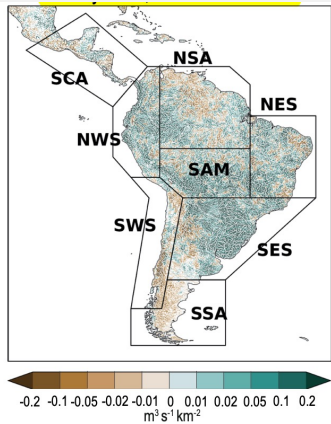Figure 12.9 | Projected changes in selected climatic impact-driver indices for Europe.

Figure 12.6 | Projected changes in selected climatic impact-driver indices for Asia.

Figure 12.8 | Projected changes in selected climatic impact-driver indices for Central and South America.
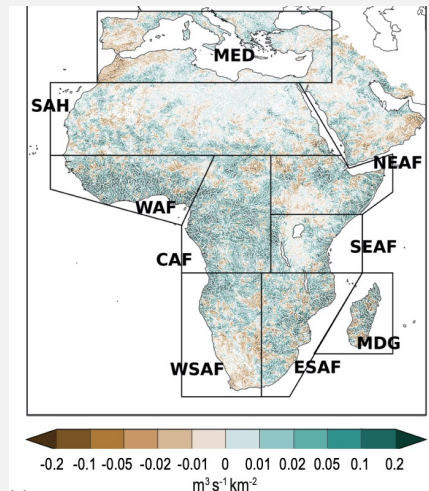

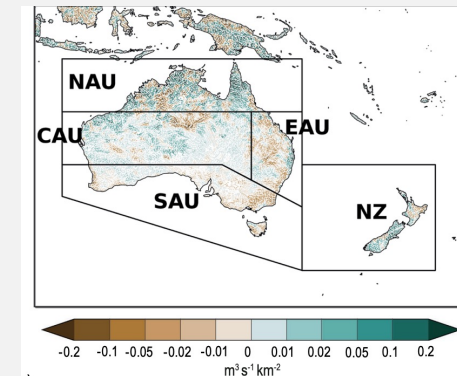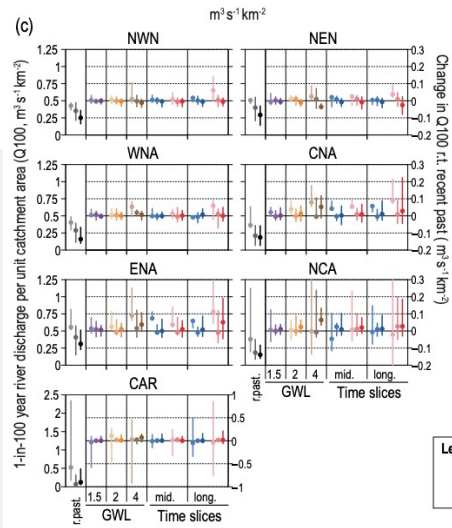Figure 12.5 | Projected changes in selected climatic impact-driver indices for Africa.

Figure 12.7 | Projected changes in selected climatic impact-driver indices for Australasia

Ranasinghe, R., Ruane, A. C., Vautard, R., Arnell, N., **Coppola**, E., Cruz, F. A., et al. (2021). "Climate Change Information for Regional Impact and for Risk Assessment," in *Climate Change 2021: The Physical Science Basis. Contribution of Working Group I to the Sixth Assessment Report of the Intergovernmental Panel on Climate Change*, eds. V. Masson-Delmotte, P. Zhai, A. Pirani, S. L. Connors, C. Péan, S. Berger, et al. (Cambridge University Press). Available at: https://www.ipcc.ch./.

Results

Future projections of river floods hazard over the multiple CORDEX-CORE domains

IPCC WGI AR6 CH12

Figure 12.9 | Projected changes in selected climatic impact-driver indices for **Europe**.

Figure 12.6 | Projected changes in selected climatic impact-driver indices for **Asia**.
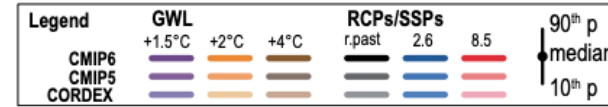
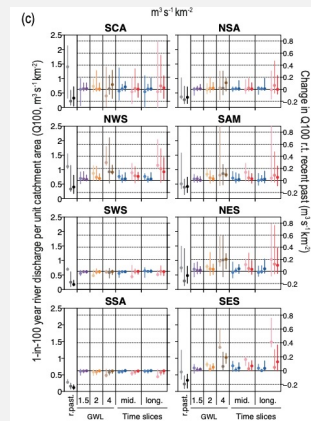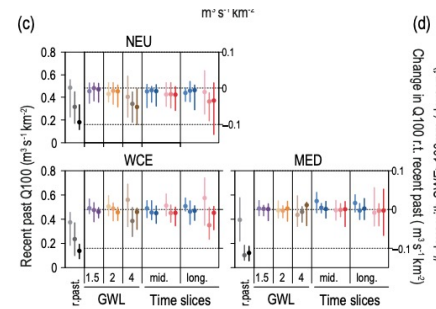Figure 12.10 | Projected changes in selected climatic impact-driver indices **North America**.

Figure 12.8 | Projected changes in selected climatic impact-driver indices for **Central and South America**.
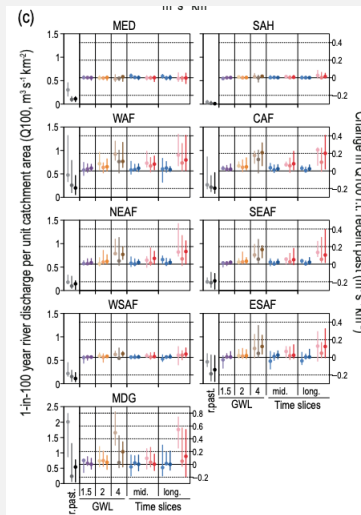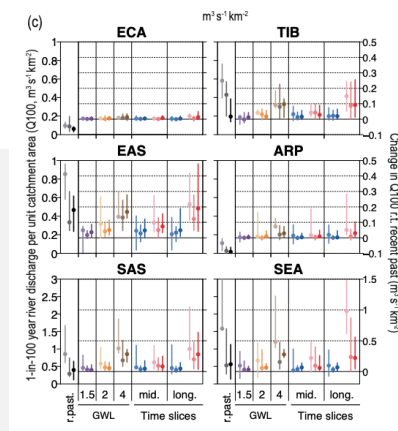
Figure 12.5 | Projected changes in selected climatic impact-driver indices for **Africa**.

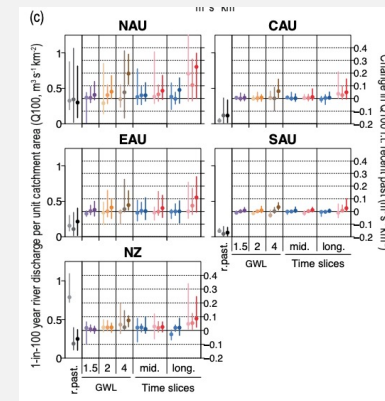Figure 12.7 | Projected changes in selected climatic impact-driver indices for **Australasia**

30

Ranasinghe, R., Ruane, A. C., Vautard, R., Arnell, N., **Coppola**, E., Cruz, F. A., et al. (2021). "Climate Change Information for Regional Impact and for Risk Assessment," in *Climate Change 2021: The Physical Science Basis. Contribution of Working Group I to the Sixth Assessment Report of the Intergovernmental Panel on Climate Change*, eds. V. Masson-Delmotte, P. Zhai, A. Pirani, S. L. Connors, C. Péan, S. Berger, et al. (Cambridge University Press). Available at: https://www.ipcc.ch./.

Results
What have we learned : caveats

1) The global warming could have an important role on the hydrological cycle. The increase of temperature and related increase of extreme precipitation phenomena could spur to an increase of disastrous floods

2) An increase in risk of floods can be observed in general over the Tropical regions, central Europe, British Islands, Australia, Japan, China, Korean peninsula, north Argentina and central-west of North America

3) On the other hand, a decrease of floods hazard can be observed over the north-east Europe, Rocky Mountains, Sierra Madre Occidental, south-east Australia, Mediterranean region, south-west Africa, Afghanistan, Turkmenistan, north Iran

4) The method has been validated over Europe but still need to be validated over the other domains

5) A statistical test to assess the robustness of the signal is needed for all the domains

What's next?
Role of clouds in a warmer climate: IPCC AR6 WGI

- Improve understanding of cloud processes due to
  - ➢better observations
  - ➢new analysis approaches
  - ➢explicit high-resolution numerical simulation of clouds.

- Improve model ability to simulate cloud behaviour due
  - ➢both to advances in computational capabilities and
  - ➢process understanding

Forster, P., T. et al., 2021: The Earth's Energy Budget, Climate Feedbacks, and Climate Sensitivity. In Climate Change 2021: The Physical Science Basis. Contribution of Working Group I to the Sixth Assessment Report of the Intergovernmental Panel on Climate Change [Masson-Delmotte, V., P. Zhai, A. Pirani, S.L. Connors, C. Péan, S. Berger, N. Caud, Y. Chen, L. Goldfarb, M.I. Gomis, M. Huang, K. Leitzell, E. Lonnoy, J.B.R. Matthews, T.K. Maycock, T. Waterfield, O. Yelekçi, R. Yu, and B. Zhou (eds.)]. Cambridge University Press, Cambridge, United Kingdom and New York, NY, USA, pp. 923–1054, doi:10.1017/9781009157896.009.

What's next?
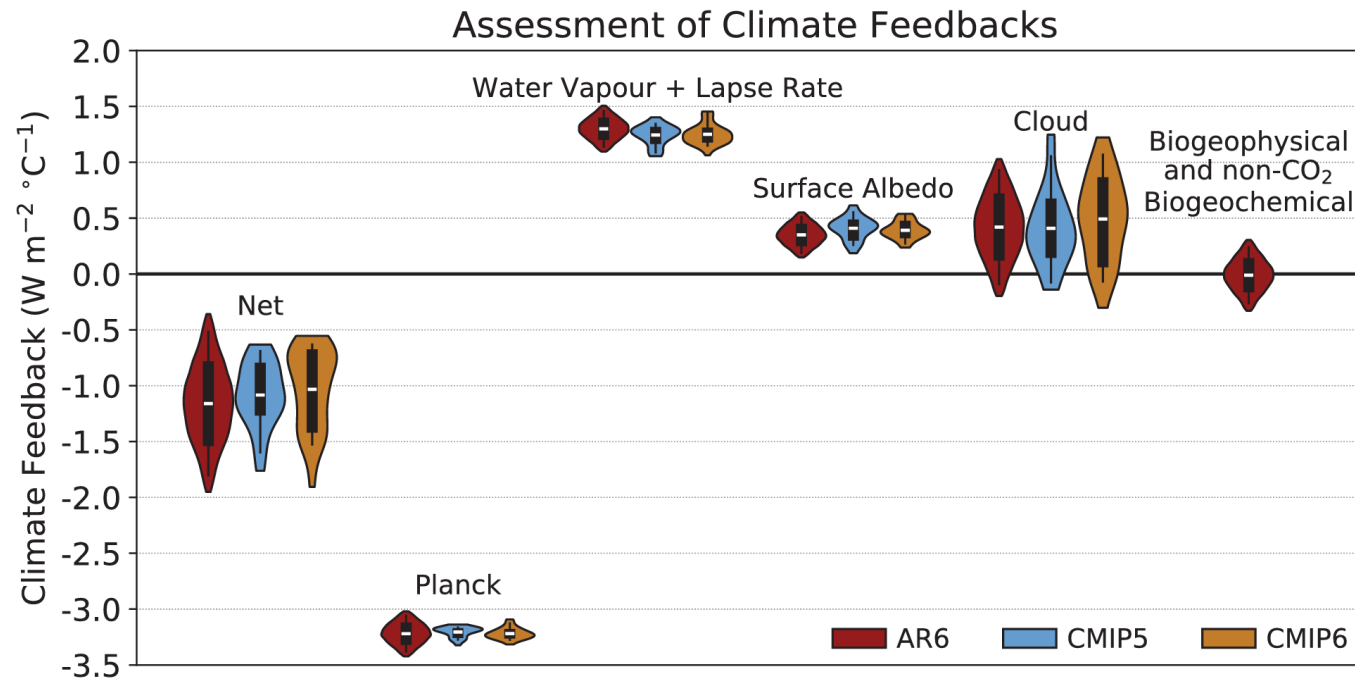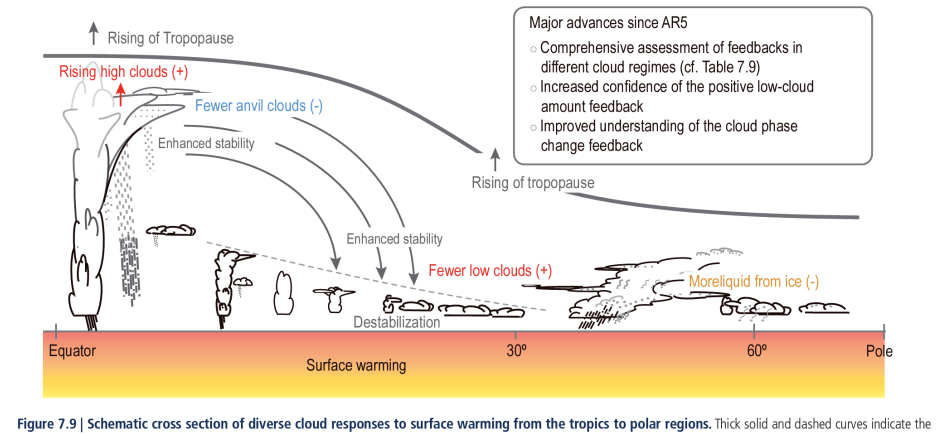## Role of clouds in a warmer climate: IPCC AR6 WGI

Figure 7.10 | Global mean climate feedbacks estimated in *abrupt4xCO2* simulations of 29 CMIP5 models (light blue) and 49 CMIP6 models (orange), compared with those assessed in this Report (red). Individual feedbacks for CMIP models are averaged across six radiative kernels as computed in Zelinka et al. (2020). The white line, black box and vertical line indicate the mean, 66% and 90% ranges, respectively. The shading represents the probability distribution across the full range of GCM/ESM values and for the 2.5–97.5 percentile range of the AR6 normal distribution. The unit is W m^{-2} °C^{-1}. Feedbacks associated with biogeophysical and non-CO_2 biogeochemical processes are assessed in AR6, but they are not explicitly estimated from general circulation models (GCMs)/Earth system models (ESMs) in CMIP5 and CMIP6. Further details on data sources and processing are available in the chapter data table (Table 7.SM.14).
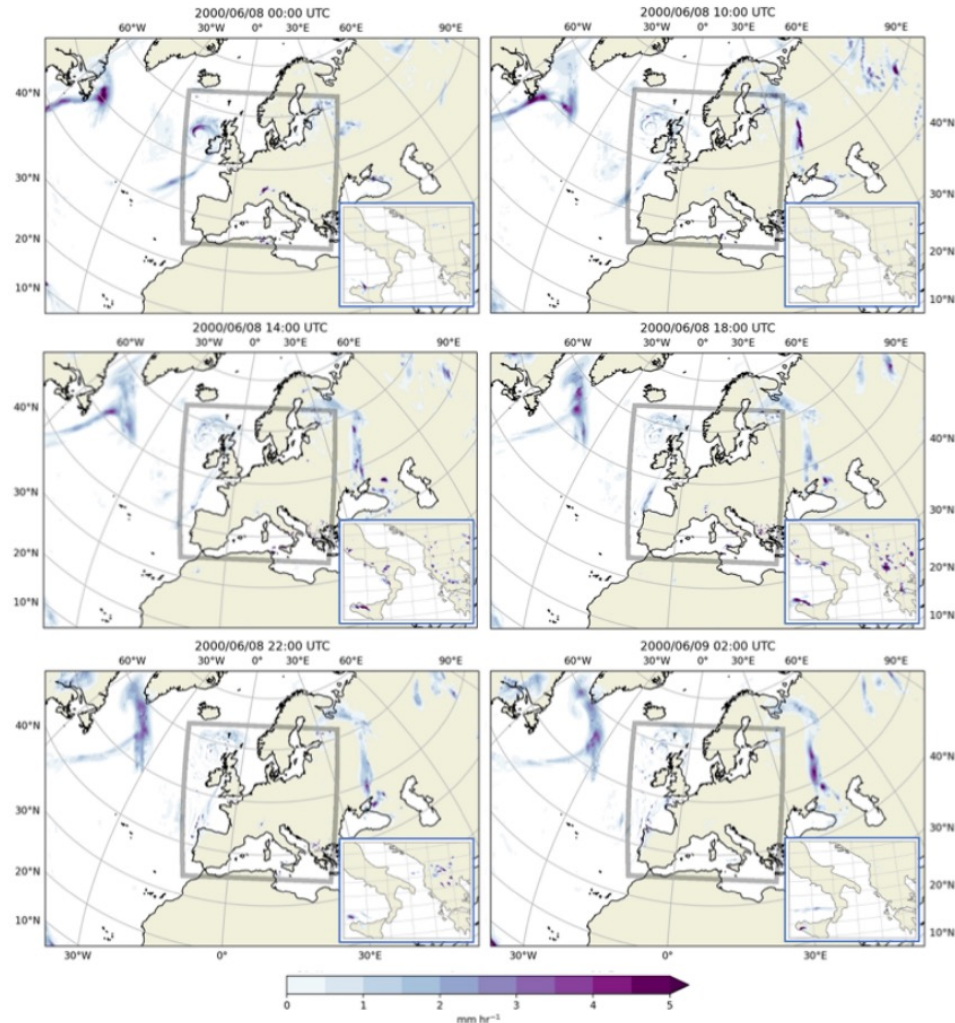
What's next?

Role of clouds in a warmer climate: IPCC AR6 WGI

Figure 7.9 | Schematic cross section of diverse cloud responses to surface warming from the tropics to polar regions. Thick solid and dashed curves indicate the

- Improve understanding on how cloud will change in a warmer climate

  ➢ the amount of **low-clouds** will reduce over the subtropical ocean, leading to less reflection of incoming solar energy → warming effect

  ➢ the altitude of **high-clouds** will rise, making them more prone to trapping outgoing energy → warming effect

  ➢ clouds in **high latitudes** will be increasingly made of water droplets rather than ice crystals. This shift from fewer, larger ice crystals to smaller but more numerous water droplets will result in more of the incoming solar energy being reflected back to space → cooling effect.

- Better understanding of how clouds respond to warming has led to more confidence than before that future changes in clouds will, overall, cause additional warming (i.e., by weakening the current cooling effect of clouds). This is called a positive net cloud feedback.
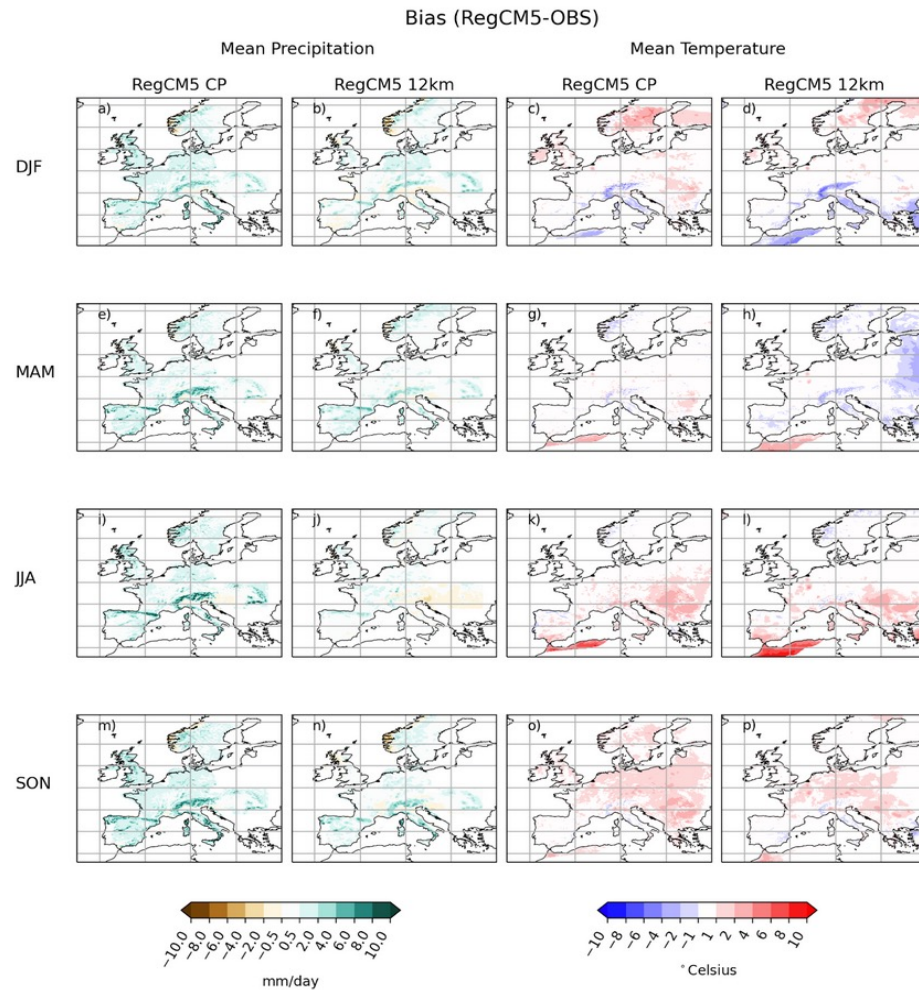
34

Forster, P., T. et al., 2021: The Earth's Energy Budget, Climate Feedbacks, and Climate Sensitivity. In Climate Change 2021: The Physical Science Basis. Contribution of Working Group I to the Sixth Assessment Report of the Intergovernmental Panel on Climate Change [Masson-Delmotte, V., P. Zhai, A. Pirani, S.L. Connors, C. Péan, S. Berger, N. Caud, Y. Chen, L. Goldfarb, M.I. Gomis, M. Huang, K. Leitzell, E. Lonnoy, J.B.R. Matthews, T.K. Maycock, T. Waterfield, O. Yelekçi, R. Yu, and B. Zhou (eds.)]. Cambridge University Press, Cambridge, United Kingdom and New York, NY, USA, pp. 923–1054, doi:10.1017/9781009157896.009.

What's next?
Very High Resolution CP-RCM
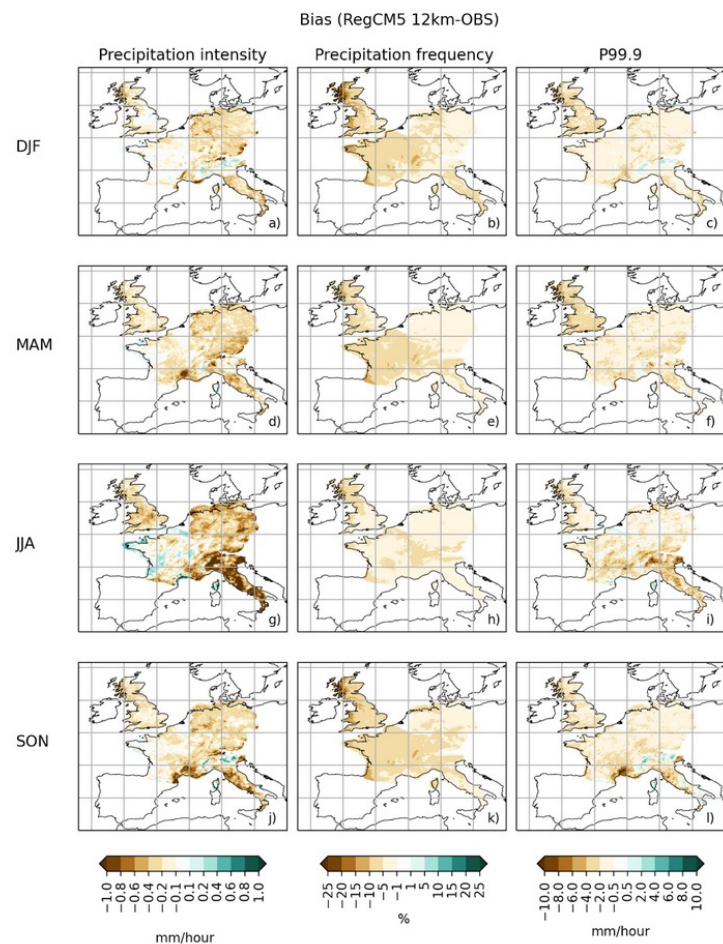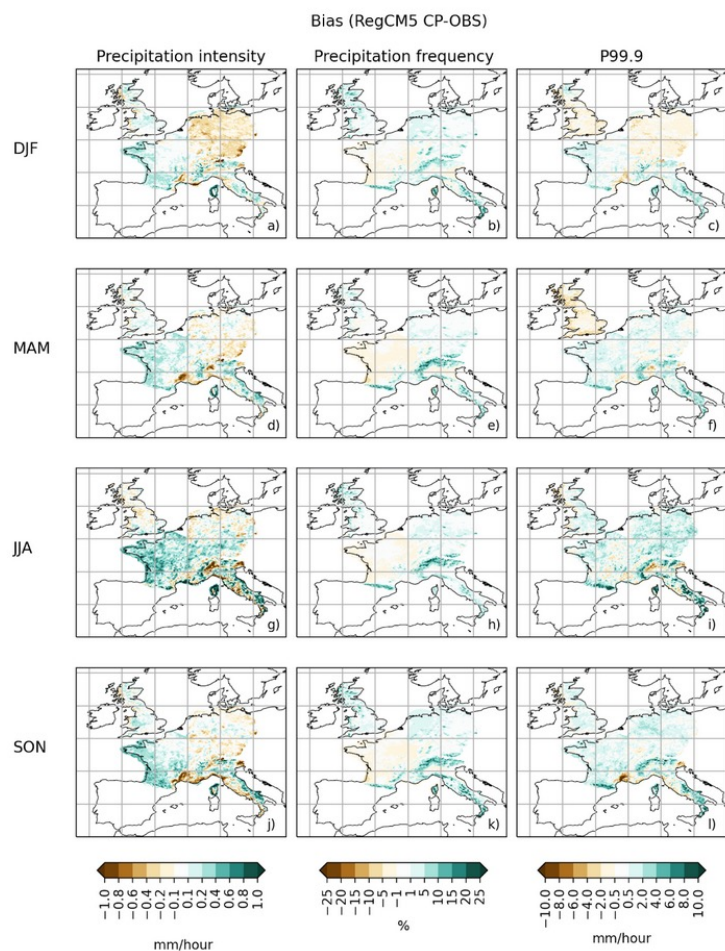
What's next?
Very High Resolution CP-RCM

Bias (RegCM5-OBS)

What's next?
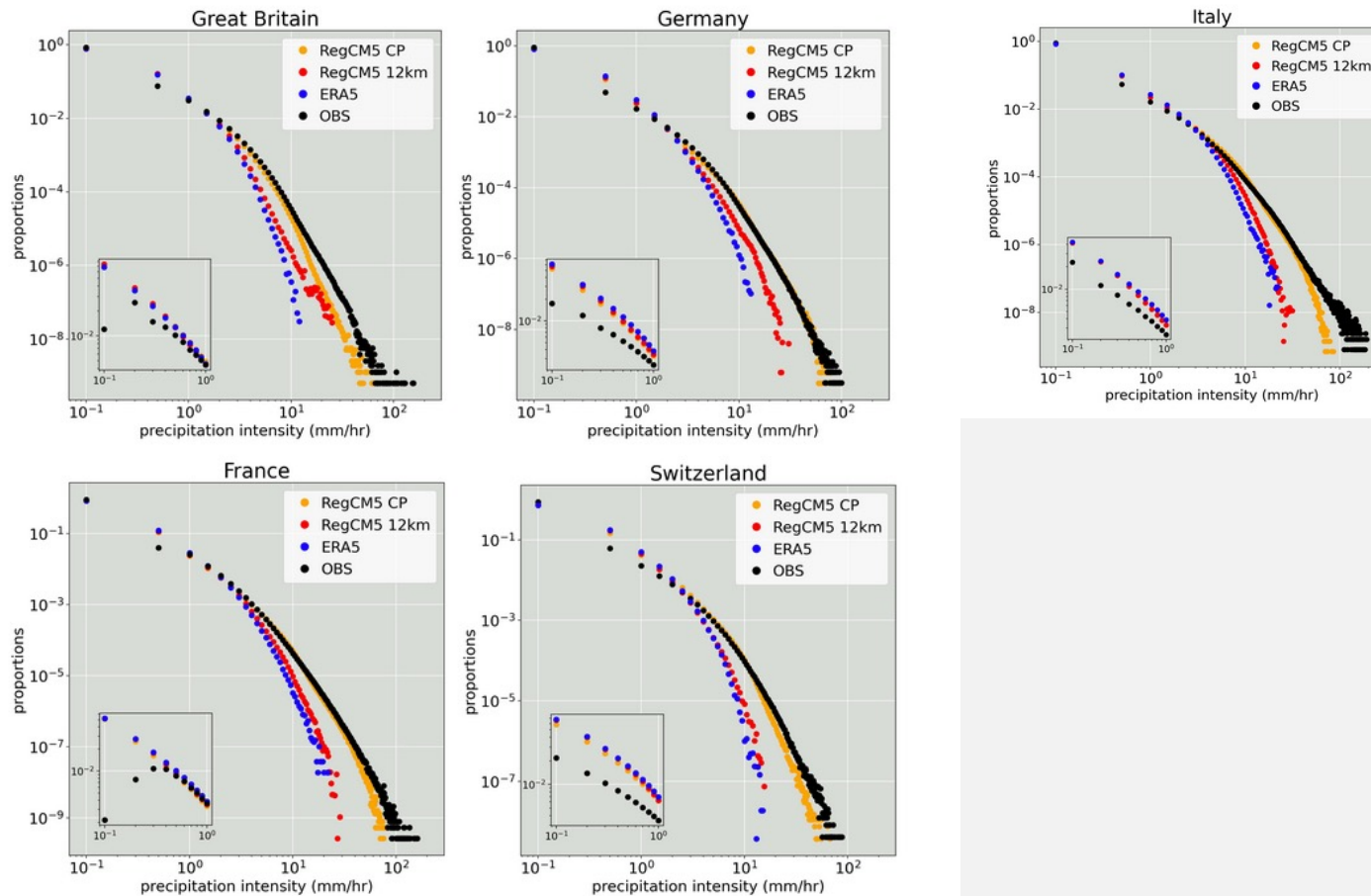## Very High Resolution CP-RCM

Intensity/ Frequency (0.05 th), P99.9- hourly
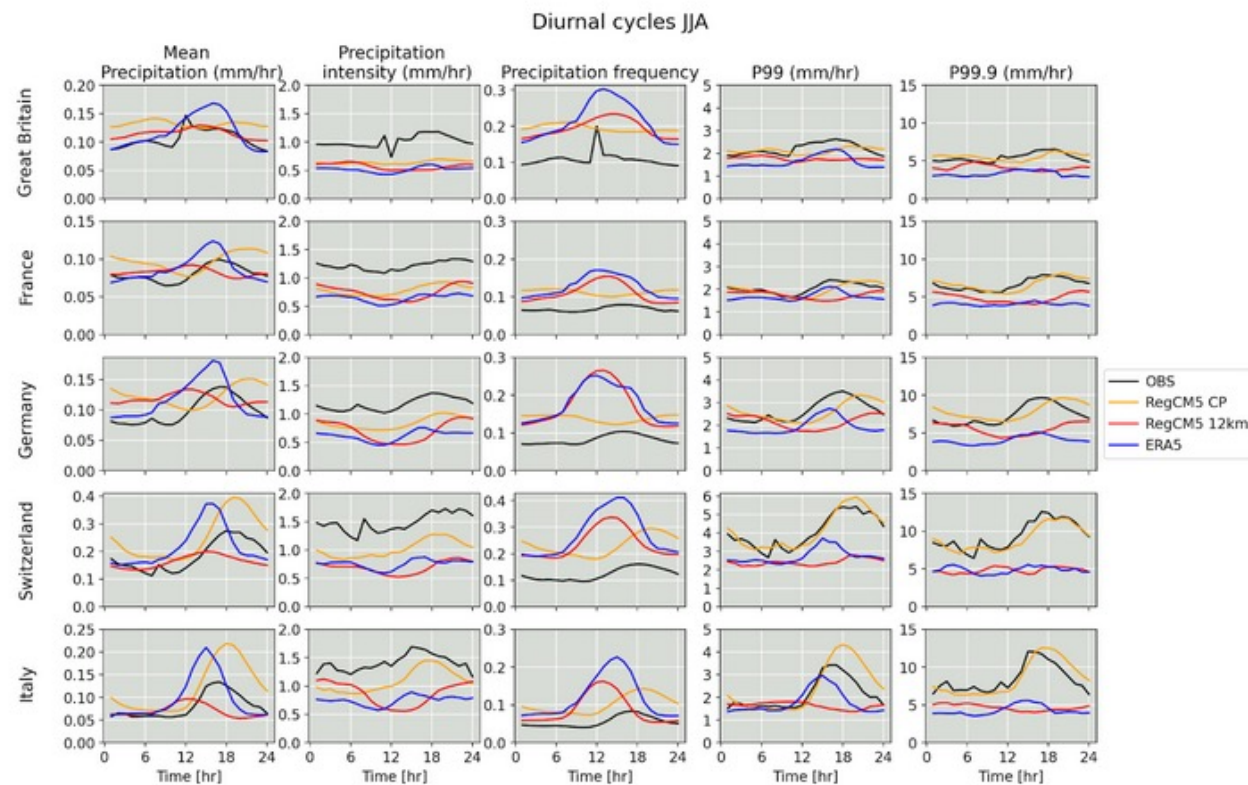
What's next?
Very High Resolution CP-RCM

Hourly PDF

What's next?
Very High Resolution CP-RCM
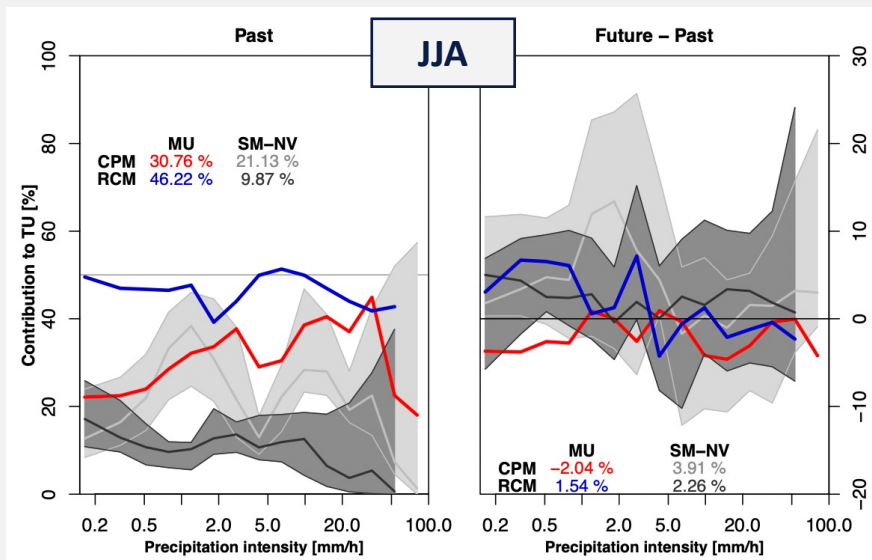
JJA diurnal cycle

Diurnal cycles JJA

Dynamical downscaling
Ensemble approach for uncertainty estimate
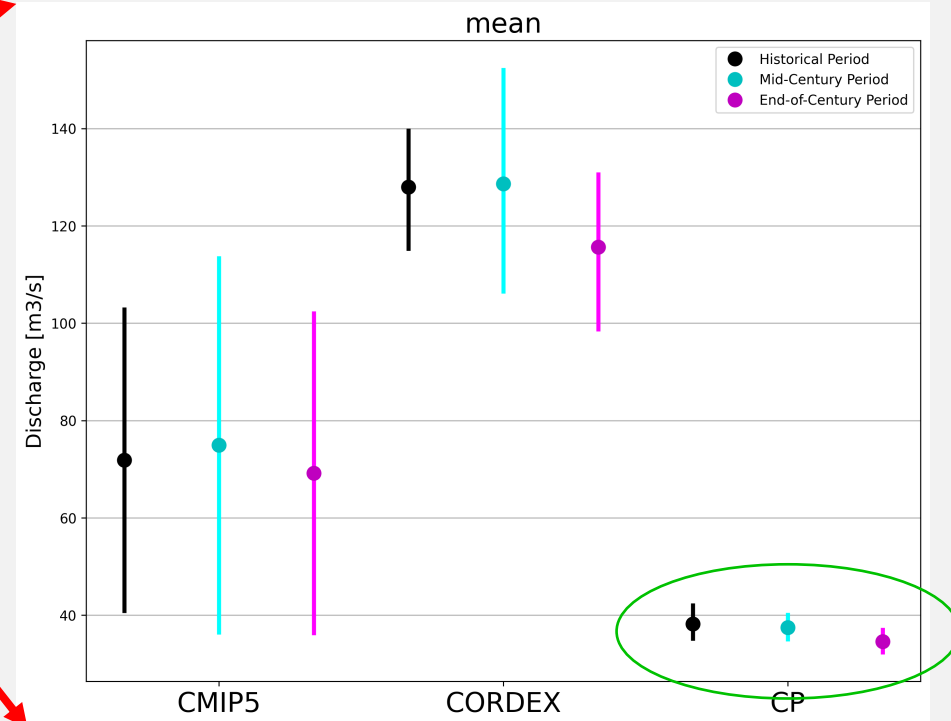### Fractional contribution of total precipitation

✓ Model uncertainties contribute to total uncertainties substantially more in RCMs than in CPMs especially for extremes

✓ The convergence in CPMs is likely to be linked to the explicit representation of convection
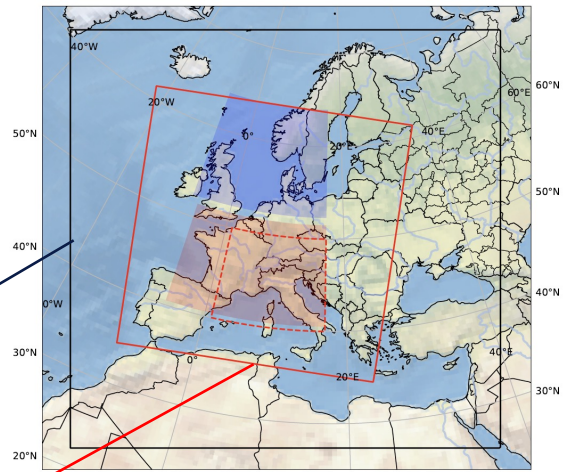
40
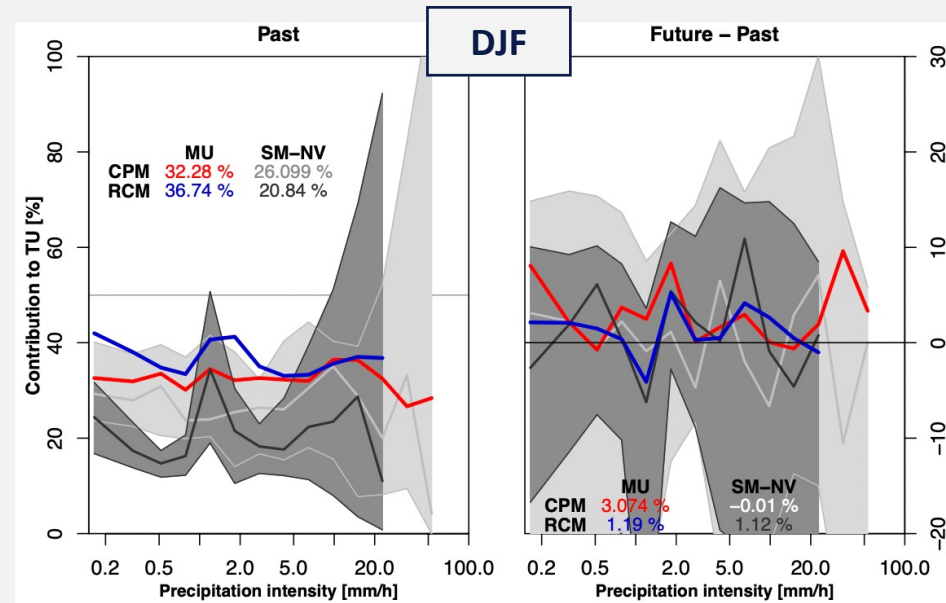
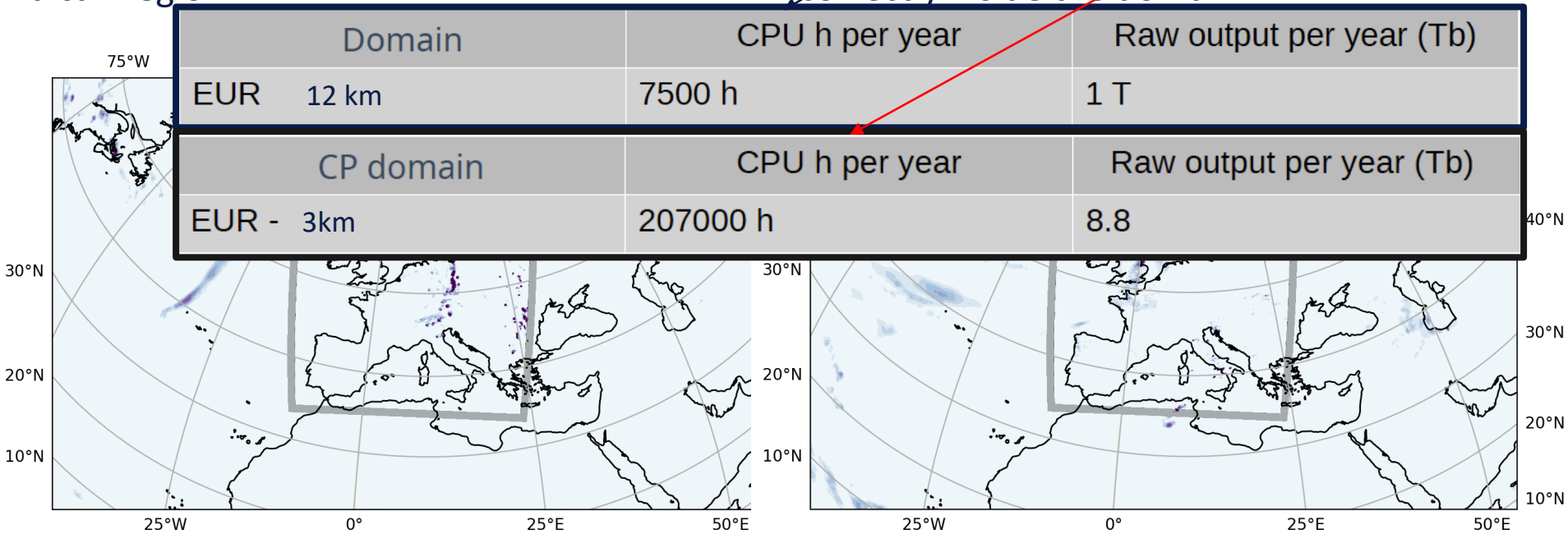# **Uncertainty propagation**
The hydrological cycle
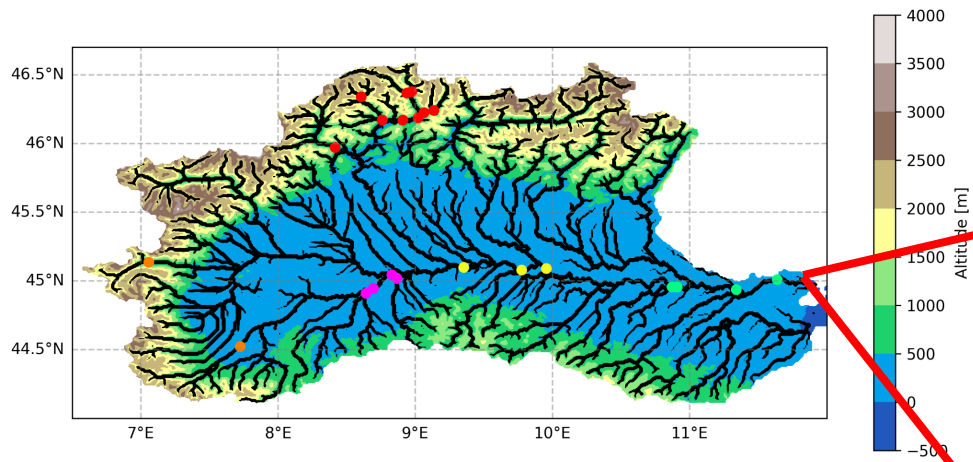
Dynamical downscaling
Convection permitting resolution

Summer convection is generated inside the domain over the Alpine chain and over the Balcan region

Fall frontal precipitation triggered by large scale dynamical forcing entering from the boundary and propagating correctly inside the domain

Domain	CPU h per year	Raw output per year (Tb)
EUR 12 km	7500 h	1 T

CP domain	CPU h per year	Raw output per year (Tb)
EUR - 3km	207000 h	8.8

42

Machine Learning Emulator

Hybrid imperfect approach (HIA) based on Graph Neural Network

CP resolution

Training   - using **REANALYSIS** input data as predictors

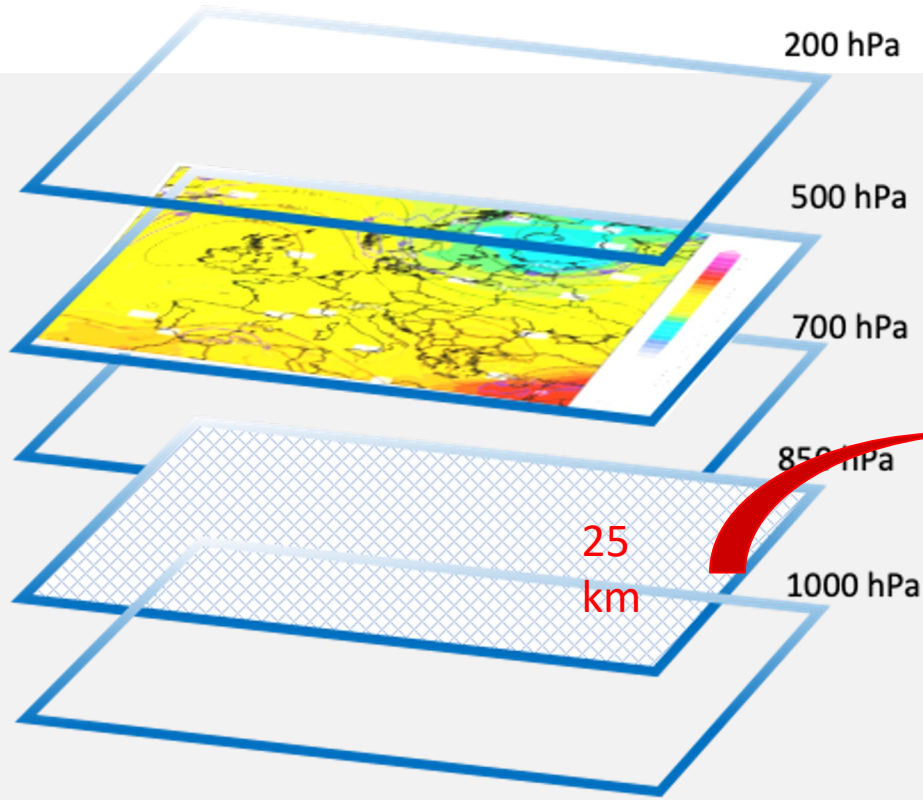**Testing :**   - using **REANALYSIS** input data as predictors → **"REAL WORLD"**

                - using **MODEL** data input data as predictors → **"MODEL WORLD"**

Machine Learning Emulator

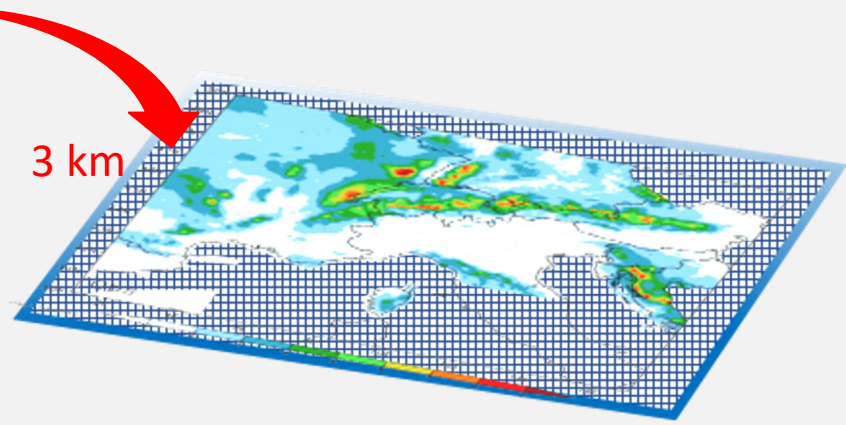## Hybrid imperfect approach (HIA) based on Graph Neural Network

The ICTP-GNN4CD emulator

	Atmosphere	Surface
"Real" world	ERA5 **25 km** (hourly)	Observations (**3 km**) (hourly or daily)
Model world (*)	Model EUR-**12km** (6-hourly)	Model ALP-**3km** (hourly)

(*) ERA-Interim driven (optimum for present days)
GCMs driven   (projections)

200 hPa

500 hPa

700 hPa

850 hPa

1000 hPa

25 km

3 km

Temperature; humidity; geopotential; winds

Precipitation

44

Machine Learning Emulator

Hybrid imperfect approach (HIA) based on Graph Neural Network
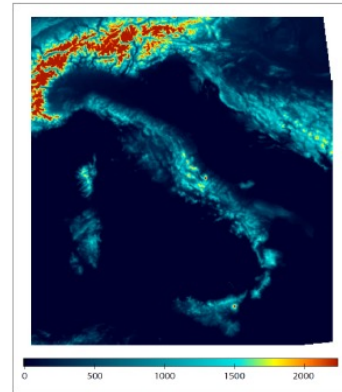
The ICTP-GNN4CD emulator
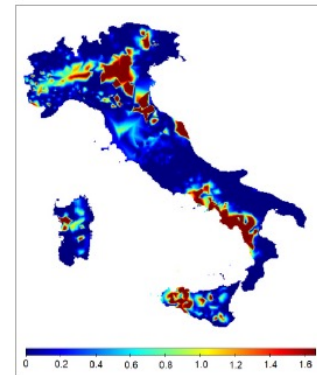
Machine Learning Emulator

Hybrid imperfect approach (HIA) based on Graph Neural Network

Training

Restricted spatial area

- Longitude x latitude = [6.5, 14.00] x [43.75, 47.25]

- Restricted target accounts for $\sim 44\%$ of the cleaned target dataset

Other set-up choices

- Years **2001-2015** (included) used for training

- Training hyper-parameters (e.g., learning rate, weight decay, batch size) defined manually, by trial and error

- Mean Square Error (MSE) loss for the Regressor

- Focal loss (FL), parameters $\alpha = 0.9$, $\gamma = 2$

$$FL(p_t) = -(1 - p_t)^\gamma \log(p_t)$$

- Adam optimizer
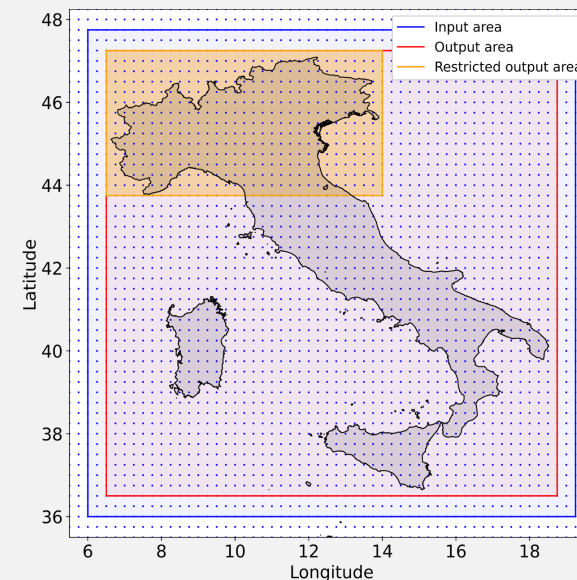
courtesy of Valentina Blasone

46

Machine Learning Emulator

Hybrid imperfect approach (HIA) based on Graph Neural Network

Network Architectures : Combination of **Convolutional + Recurrent + Graph** neural networks
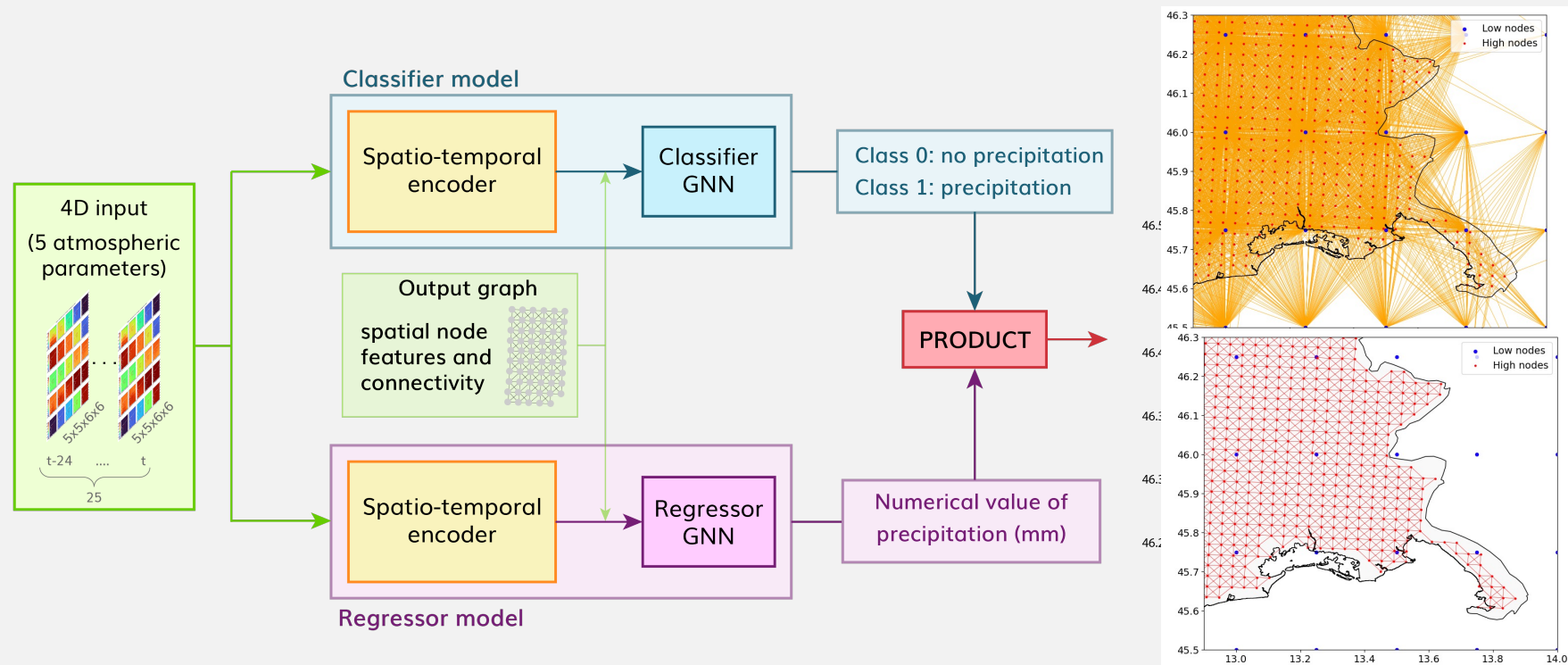
courtesy of Valentina Blasone

47

Machine Learning Emulator

Hybrid imperfect approach (HIA) based on Graph Neural Network

"MODEL WORLD" RESULTS
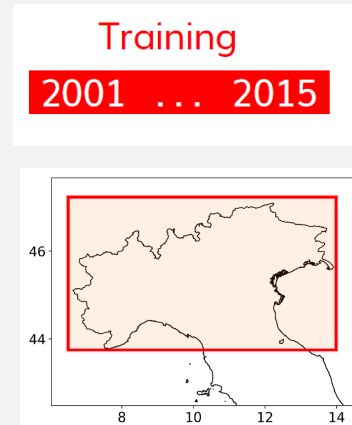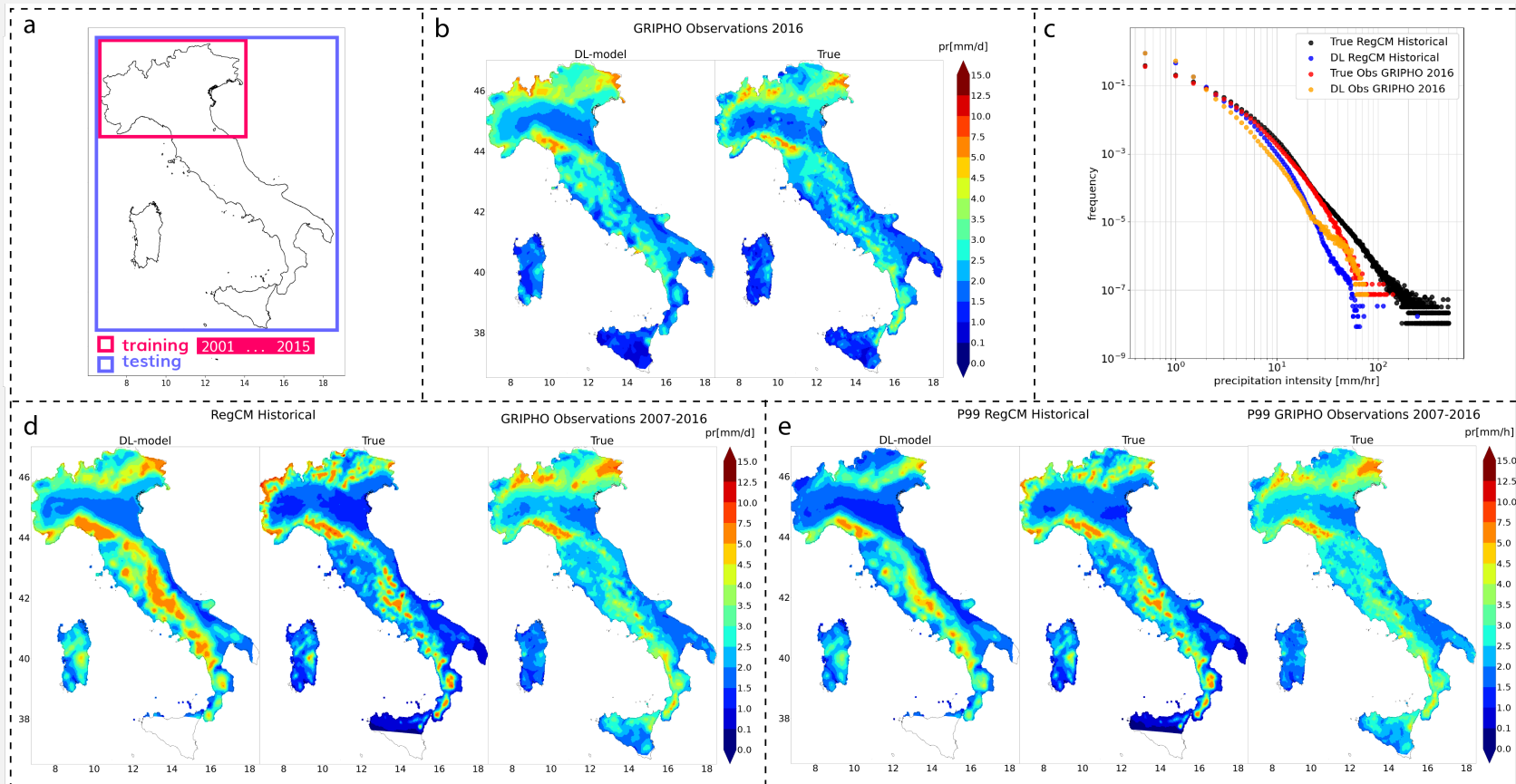
courtesy of Valentina Blasone

48

Machine Learning Emulator

Hybrid imperfect approach (HIA) based on Graph Neural Network

The ICTP-GNN4CD emulator : Validation with future Model data
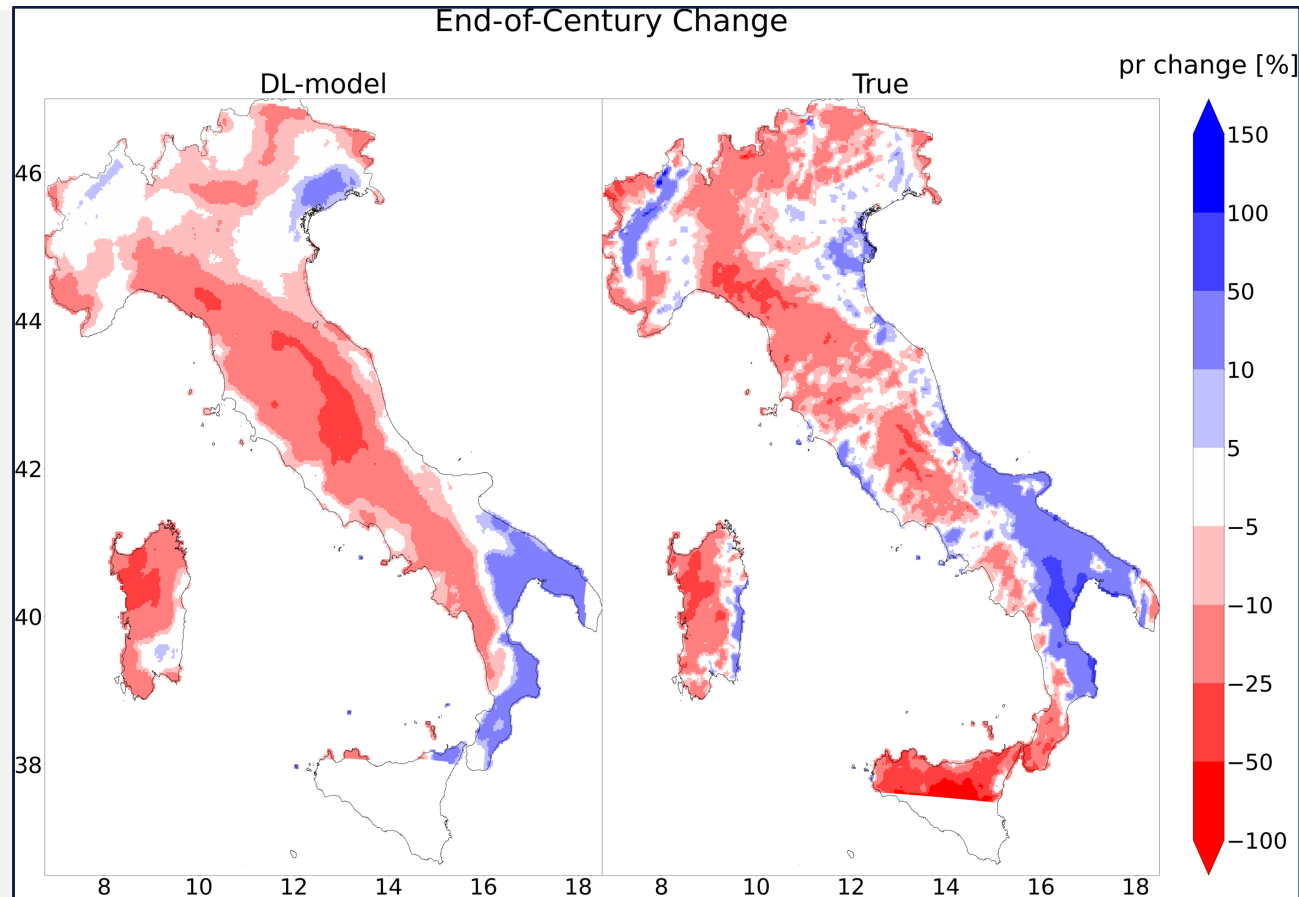
courtesy of Valentina Blasone

Machine Learning Emulator
Hybrid imperfect approach (HIA) based on Graph Neural Network

The ICTP-GNN4CD emulator : Validation with future Model data
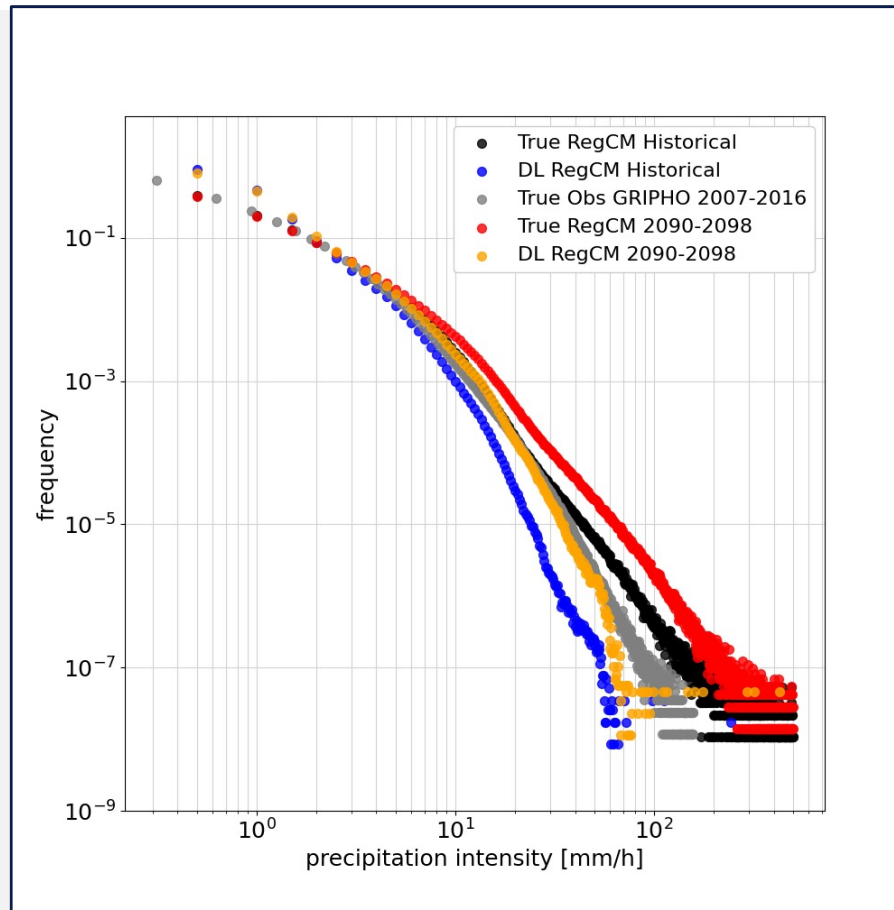
PhD position opened

PhD Programme in Earth science, fluid-dynamics and mathematics.
Interactions and methods

at the University of Trieste, Italy and in collaboration with OGS and
the Abdus Salam International Centre for Theoretical Physics (ICTP).

https://portale.units.it/en/research/phd/programmes/earth-science

This year, the PhD program is offering 6 scholarships:

- 5 scholarships in any topic related to the PhD sectors/research lines

- 1 scholarship funded by ICTP on the general subject of climate
variability and change. This scholarship is reserved for applicants from
countries that are NOT
included in the World Bank's list of 'High-income economies'.

Deadline for applications: 13 June 2024.

Thanks

51

Machine Learning Emulator

Hybrid imperfect approach (HIA) based on Graph Neural Network

- Test the ML model with others CP-RCM

- Test the ML in the Hard transferability framework

- Include extra inputs: relative humidity, GHG concentration -→ warmer world

- Land use to improve the spatial transferability

Machine Learning Emulator
Open questions

- Transferability

- Performance for extremes and out-of-sample events

- Evaluations metrics

- Emulators as useful to augment dynamical simulations

53

References

Babaousmail H, Hou R, Gnitou GT, Ayugi B (2021) Novel statistical downscaling emulator for precipitation projections using deep Convolutional Autoencoder over
Northern Africa. Journal of Atmospheric and Solar-Terrestrial Physics 218:105,614, DOI 10.1016/J.JASTP.2021.105614

Ban, N., Caillaud, C., Coppola, E., Pichelli, E., Sobolowski, S., Adinolfi, M., ... & Zander, M. J. (2021). The first multi-model ensemble of regional climate simulations at kilometer-scale resolution, part I: evaluation of precipitation. Climate Dynamics, https://doi.org/10.1007/s00382-021-05708-w, 1-28.

Baño-Medina J, Manzanas R, Gutierrez JM, Gutiérrez JM (2020) Configuration and intercomparison of deep learning neural models for statistical downscaling. Geoscientific Model Development 13(4):2109–2124, DOI 10.5194/gmd-13-2109-2020, URL https://gmd.copernicus.org/articles/13/2109/2020/

Bano-Medina et al., Transferability and explainability of deep learning emulators for regional climate model projections: Perspectives for future applications (2023). Submitted to Artificial Intelligence for the Earth Systems https://doi.org/10.1007/s00382-022-06343-9

Berthou S, Kendon EJ, Chan SC, Ban N, Leutwyler D, Schär C, Fosser G (2020) Pan-European climate at convection-permitting scale: a model intercomparison study. Climate Dynamics 55(1-2):35–59, DOI 10.1007/s00382-018-4114-6

Boé J, Somot S, Corre L, Nabat P (2020) Large discrepancies in summer climate change over Europe as projected by global and regional climate models: causes and consequences. Climate Dynamics DOI 10.1007/s00382-020-05153-1

Boé J, Mass A, Deman J (2022) A simple hybrid statistical–dynamical downscaling method for emulating regional climate models over Western Europe. Evaluation, application, and role of added value? Climate Dynamics 2022 1:1–24, DOI 10.1007/S00382-022-06552-2, URL

Coppola, E., Sobolowski, S., Pichelli, E. et al. (2020). A first-of-its-kind multi-model convection permitting ensemble for investigating convective phenomena over Europe and the Mediterranean. Clim Dyn 55, 3–34. https://doi.org/10.1007/s00382-018-4521-8

Coppola E, Nogherotto R, Ciarlo' JM, Giorgi F, van Meijgaard E, Kadygrov N, Iles C, Corre L, Sandstad M, Somot S, Nabat P, Vautard R, Levavasseur G, Schwingshackl C, Sillmann J, Kjellström E, Nikulin G, Aalbers E, Lenderink G, Christensen OB, Boberg F, Sørland SL, Demory ME, Bülow K, Teichmann C, Warrach-Sagi K, Wulfmeyer V (2021) Assessment of the European Climate Projections as Simulated by the
Large EURO-CORDEX Regional and Global Climate Model Ensemble. Journal of Geophysical Research: Atmospheres 126(4):e2019JD032,356, DOI 10.1029/2019JD032356, URL https://onlinelibrary.wiley.com/doi/full/10.1029/2019JD032356https://onlinelibrary.wiley.com/doi/abs/10.1029/2019JD032356https://agupubs.onlinelibrary.wiley.com/doi/10.1029/2019JD032356

Doury A, Somot S, Gadat S, Ribes A, Corre L (2022) Regional climate model emulator based on deep learning: concept and first evaluation of a novel hybrid downscaling approach. Climate Dynamics 1:1–29, DOI 10.1007/S00382-022-06343-9/FIGURES/16, URL https://link.springer.com/article/10.1007/s00382-022-06343-9

Evin G, Somot S, Hingray B (2021) Balanced estimate and uncertainty assessment of European climate change using the large EURO-CORDEX regional climate model ensemble. Earth System Dynamics Discussions (March):1–40, DOI 10.5194/esd-2021-8
Giorgi F (2019) Thirty Years of Regional Climate Modeling: Where Are We and Where Are We Going next? Journal of Geophysical Research: Atmospheres 124(11):5696–5723, DOI 10.1029/2018JD030094
Gutiérrez JM, Maraun D, Widmann M, Huth R, Hertig E, Benestad R, Roessler O, Wibig J, Wilcke R, Kotlarski S, San Martín D, Herrera S, Bedia J, Casanueva A, Manzanas R, Iturbide M, Vrac M, Dubrovsky M, Ribalaygua J, Pórtoles J, Räty O, Räisänen J, Hingray B, Raynaud D, Casado MJ, Ramos P, Zerenner T, Turco M, Bosshard T, Štěpánek P, Bartholy J, Pongracz R, Keller DE, Fischer AM, Cardoso RM, Soares PM, Czernecki B, Pagé C (2019) An intercomparison of a large ensemble of statistical downscaling methods over Europe: Results from the VALUE perfect predictor cross-validation experiment. International Journal of Climatology 39(9):3750–3785, DOI 10.1002/joc.5462

Huth R, Mikšovský J, Štěpánek P, Belda M, Farda A, Chládová Z, Pišoft P (2015) Comparative validation of statistical and dynamical downscaling models on a dense grid in central Europe: temperature. Theoretical and Applied Climatology 120(3-4):533–553, DOI 10.1007/s00704-014-1190-3

Laprise R, de Elía R, Caya D, Biner S, Lucas-Picher P, Diaconescu E, Leduc M, Alexandru A, Separovic L (2008) Challenging some tenets of Regional Climate Modelling Network for Regional Climate Modelling and Diagnostics. Meteorol Atmos Phys 100:3–22, DOI 10.1007/s00703-008-0292-9

Maraun D, Wetterhall F, Ireson AM, Chandler RE, Kendon EJ, Widmann M, Brienen S, Rust HW, Sauter T, Themel M, Venema VK, Chun KP, Goodess CM, Jones RG, Onof C, Vrac M, Thiele-Eich I (2010) Precipitation downscaling under climate change: Recent developments to bridge the gap between dynamical models and the end user. Reviews of Geophysics 48(3), DOI 10.1029/2009RG000314

Michelangeli PA, Vrac M, Loukos H (2009) Probabilistic downscaling approaches: Application to wind cumulative distribution functions. Geophysical Research Letters 36(11):2–7, DOI 10.1029/2009GL038401

Pichelli, E., Coppola, E., Sobolowski, S., Ban, N., Giorgi, F., Stocchi, P., ... & Vergara-Temprado, J. (2021). The first multi-model ensemble of regional climate simulations at kilometer-scale resolution part 2: historical and future simulations of precipitation. Climate Dynamics, 56(11), https://doi.org/10.1007/s00382-021-05657-4, 3581-3602

Ronneberger O, Fischer P, Brox T (2015) U-net: Convolutional networks for biomedical image segmentation. In: Lecture Notes in Computer Science (including subseries Lecture Notes in Artificial Intelligence and Lecture Notes in Bioinformatics), vol 9351, pp 234–241, DOI 10.1007/978-3-319-24574-4_28